A Simple Procedure to Determine Surface Charging Parameters in Aqueous Solutions

Theresa Feltes and Melanie Timmons
under the supervision of
Dr. John Regalbuto[1]

The measurement technique of "equilibrium pH at high oxide loading" was used to study the pH shifts associated with several types of alumina, silica, and carbon. The use of these substances as catalyst supports necessitates a detailed understanding of the pH shift and its relationship to surface charge. These materials were placed in aqueous solutions of varying initial pH to yield final pH measurements, which were then compared to a simple non-Nernstian model. The ultimate goal of this project is to use numerical optimization techniques to determine several surface-charging parameters including PZC, DpK, Ns. However, the current work is based on a primitive trial and error technique for the determination of these values.

INTRODUCTION

The most general purpose for this research is to make a more effective catalyst. One way to do this is to utilize a support that supplies a better dispersion of the catalyst. In order for a catalyst to achieve an optimal uptake onto an oxide surface, the effect of the pH shift (i.e. change in pH of a solution before and after oxide addition) of the aqueous solution must be studied and certain charging parameters must be determined. The pH shift may be obtained from the surface part of the non-Nerstian Revised Physical Adsorption Model (RPA) (6). The model consists of the simultaneous solution of three equations: the Surface Ionization model, the Gouy-Chapman electric double layer model, and a simple Proton Balance. The critical parameters for this model are the point of zero charge (PZC, the pH of the solution when the net oxide surface charge is zero), the

[1] To whom correspondence should be directed.

difference between the ionization constants[2] K_1 and K_2, which often expressed as ΔpK or DpK (= pK2 – pK1), and the surface density of chargeable sites, Ns (OH groups/nm^2) (6).

The critical parameters for the RPA model may be determined with a variety of different methods. The value of Ns may be ascertained from isotope exchange, acid-base titration, infrared spectroscopy, and chemical reactions (6). While methods such as potentiometric titration and mass titration were used to determine the value of DpK (6). However, a more simple method to determine DpK, Ns, and even PZC may exist. It is our objective to determine these parameters from this new method and access their reliability.

The PZC of the oxide may be the most important parameter since it is the pH around which a strong buffering effect is observed (6). The buffering effect is seen through the plateau on a pH final (pH after oxide addition) vs. pH initial graph. The oxide surface becomes protonated (deprotonated) when the initial pH is below (above) the afore-mentioned plateau region (6). Refer to the theory section for a more detailed discussion of this phenomenon. It should be noted that the DpK is also of utmost importance since it is inversely proportional to the length of the PZC plateau (6).

The current the work is an extension of that completed by Park and Regalubuto who performed tests at incipient wetness, where is the amount of liquid added just equals the water accessible pore volume of the solid and is therefore the highest possible mass content (6). This extension includes experiments at various surface loadings where a final pH was measured over a range of initial pH solutions.

[2] To be discussed in further detail under the theory section.

THEORY

Background

Oxide ions are strong bases (5). Thus, in aqueous solutions, they become neutralized by water to form hydroxyl groups (5). The hydroxyl groups on the surface of an amphoteric oxide then become protonated or deprotonated, which leads the solution pH increasing or decreasing (6). In other words, as oxides in an acidic (basic) pH become protonated (deprotonated) the solution, which supplies (consumes) protons, becomes more basic (acidic) (6).

This general concept is shown in the diagram below:

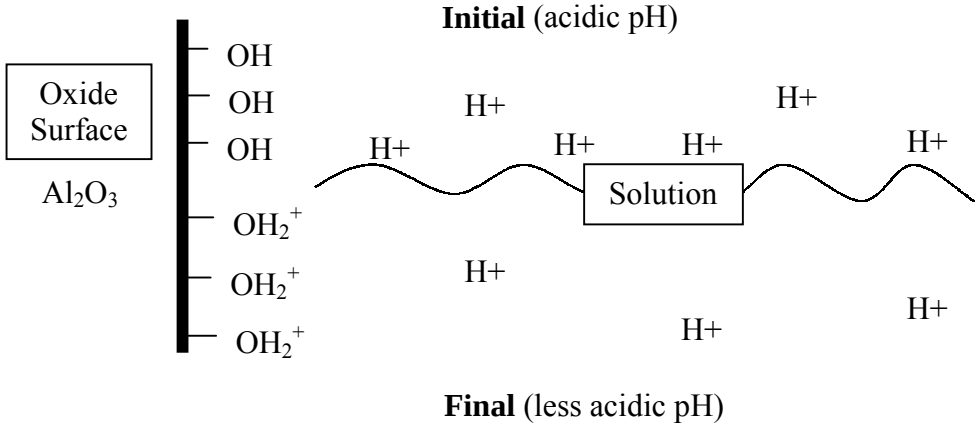

Figure 1. A visual representation of a pH shift. The protons from the solution become associated with the oxide surface creating an oxide surface charge and resulting in a decreased acidy.

Note from the final solution that the oxide surface is now charged. The surface charge is used to attract different ionic metal complexes. For example, a positive surface charge would more strongly attract $PtCl_6^{2-}$ (chloroplatinic acid) and a negative surface charge would more strongly attract $(NH_3)_4Pt^{2+}$ (tetraammineplatinum(II) chloride hydrate) (5).

The surface ionization constants associated with the before mentioned protonation/deprotonation of an amphoteric oxide surface, such as alumina, may be seen

below. Also, note that the equations denote the concentration of the positive $[MOH_2^+]$, negative $[MO^-]$, and neutral [MOH] surface groups on the metal solid, M, as well as the proton concentration $[H_s^+]$ located on the oxide surface (5).

$$K_1 = \frac{[MOH] * [H_s^+]}{[MOH_2^+]} \qquad K_2 = \frac{[MO^-] * [H_s^+]}{[MOH]}$$

These constants were derived from the charging mechanism expressed as

$$[MOH_2^+] \overset{K_1}{=} [MOH] + [H_s^+] \qquad [MOH] \overset{K_2}{=} [MO^-] + [H_s^+]$$

RPA Model

The final pH of the solution is therefore a very important parameter, which may be determined using the surface part of the RPA model. The model is based on the simultaneous solutions of three equations, which will now be discussed in detail.

First, the surface ionization model states the surface charge is equal to the fraction of positively charged sites minus the fraction of negatively charged sites (6).

$$\frac{\sigma_o}{(\Gamma_t * F)} = \frac{[MOH_2^+] - [MO^-]}{[MOH_2^+] + [MOH] + [MO^-]}$$

When expressed in variables used within the model the following equation is obtained:

$$\sigma_o = \left[\frac{\frac{Hf \cdot e^{-\frac{\eta \cdot \Psi_o}{k \cdot T}}}{K_1} - \frac{K_2 \cdot e^{\frac{\eta \cdot \Psi_o}{k \cdot T}}}{Hf}}{\left(\frac{Hf \cdot e^{-\frac{\eta \cdot \Psi_o}{k \cdot T}}}{K_1} + 1 + \frac{K_2 \cdot e^{\frac{\eta \cdot \Psi_o}{k \cdot T}}}{Hf} \right)} \right] \cdot F \cdot \Gamma_t$$

Surface Ionization Model
σ_o = Surface Charge (Unknown)
Ψ_o = the Surface Potential (Unknown)
H_f = Final Proton Concentration (Unknown)
η = the electron charge ($1.6*10^{-19}$ C)
k = Boltzman Constant ($1.38066*10^{-23}$J/K)
T = Temperature (298K)
$K_1 = 10^{-(PZC - 0.5\Delta pK)}$
$K_2 = 10^{-(PZC + 0.5\Delta pK)}$
F = Faraday constant ($9.649*10^4$ C/mole)
Γ_t = the density of charged sites ($10^{-5}*N_s/6.02$ moles/m^2)
N_s = density of hydroxyl groups

The second equation is derived from the original Gouy-Chapman equation. It relates charge and potential in the electric double layer (6). The electric double layer consists of a layer of charge on the oxide particle's surface and another layer of opposite charge in the surrounding solution (5).

$$\sigma_o = \sqrt{8 \cdot \varepsilon \cdot \varepsilon_o \cdot k \cdot T \cdot n_o} \cdot \sinh\left(\frac{\eta \cdot \Psi_o}{2 \cdot k \cdot T}\right)$$

Gouy-Chapman
σ_o = Surface Charge (Unknown)
Ψ_o = the Surface Potential (Unknown)
ε = the relative dielectric constant of the solution (78.41)
ε_o = the permittivity of vacuum ($8.854*10^{-12}$ C^2/Nm^2)
k = Boltzman Constant ($1.38066*10^{-23}$J/K)
T = Temperature (298K)
n_o = number of electrolyte ions per unit volume (M_{ionic} * Avegadros Number)
η = the electron charge ($1.6*10^{-19}$ C)

The final equation is simple a proton balance.

Proton Balance Equation
σ_o = Surface Charge (Unknown)
H_f = Final Proton Concentration (Unknown)
F = Faraday constant ($9.649*10^4$ C/mole)
w = the mass concentration of oxide (varies g/L)
s_{areaO} = the specific surface area of the oxide (varies m^2/g)
γ = activity coefficient, from the extended Debye-Huckel equation
c_o = the standard concentration (1 mole/L)
pH = Initial pH of solution

$$\sigma_o = \frac{F}{w \cdot s_{areaO}}\left[\left[10^{-pH} - 10^{-(14-pH)}\right] + \left(\frac{10^{-14}}{Hf} - Hf\right)\cdot\left(\frac{c_o}{\gamma}\right)\right]$$

Converts from a M to a charge

Initial H+ concentration in solution

Initial OH- concentration in solution

Final OH- concentration in solution

Final H+ concentration in solution

Takes the activity coefficient into account

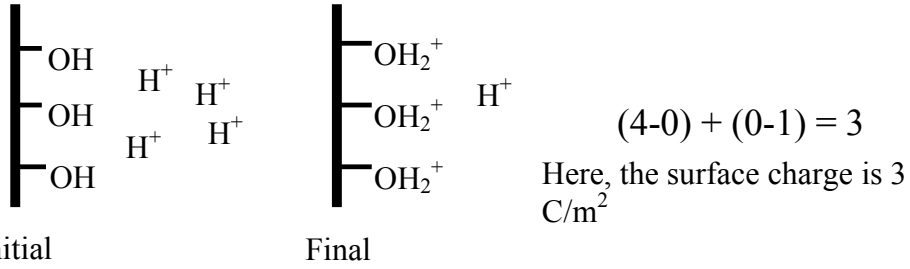

(4-0) + (0-1) = 3

Here, the surface charge is 3 C/m^2

Figure 2. A visual representation of a proton balance.

Ns Values

The Ns value was just stated to be an unknown. However, as stated previously, this value may be determined from other experimental methods. Unfortunately, literature values for this parameter vary greatly. Below is a table of several values accumulated from a brief literature search.

Sample	Ns (OH/nm^2)	Surface Area (m^2/g)	Experimental Method	Temperature (^oC)	Source
γ-Al_2O_3	8.5	230	NMR Spectroscopy	N/A	1
	8.3	N/A	Rehydration	100	2
	8.49102	N/A	Titrium exchange w/ hydroxyl protons	N/A	3
	12.52576	N/A	Crystallographic Calculations	N/A	3
	9.033	N/A	Grignard		3
	12.044	N/A	Dehydration by Heating		3
	1.32484	N/A	Surface acid-base, ion-exchange reactions for saturation	N/A	3
	1.029762	N/A	Surface acid-base, ion-exchange reactions for saturation	N/A	3
	19.2704	155	Grignard	N/A	3
θ-Al_2O_3	No Information At This Time				
α-Al_2O_3	No Information At This Time				
Fumed Silica	4	N/A	Thermo gravity	N/A	4
	3.8 ± 0.2	200	Thermo gravity	N/A	4
	17 ± 2*	200	NMR Spectroscopy	N/A	4
	4.4 ± 0.4	200	Raman Spectroscopy	N/A	4
Precipitated Silica	4.2	180	Flame Hydrolysis (B.E.T)	< 300	5
	4.6	N/A	Hydration/Re hydration	N/A	5
	4.4	N/A	Stöber Theoretical	N/A	5
	3.75	N/A	Stöber Experimental	N/A	5
	15 ± 1	175	Thermo gravity	N/A	4
	13.5 ± 1	175	NMR Spectroscopy	N/A	4
	2.4088	477	Grignard	100	3
	2.52924	N/A	Dehydration by Heating	100	3
All Carbon	No Information At This Time				

* Note this Data was proven incorrect

(1) Kraus, H., and Prins, R., *J. of Catal.* **164**, 260 (1996).
(2) Peri, J. B., *J. Phys. Chem.*, **69**, 211 (1965)
(3)Tamura, H., Tanaka, A., Mita, K., Furuichi, R., *J. Colloid Interface Sci.,* **209**, 225 (1999)
(4) Humbert, B., *J. of Non-Crystalline Solids*, **191**, 29 (1995)
(5) Fripiat, J.J., and Uytterhoeven, J., *J. Phys. Chem.*, **66**, 800 (1961)

Figure 3. A compilation of Ns values attained from various literary works.

PZC Deviation

Previously, it was noted that the PZC corresponds to the point where the oxide surface charge is neutral, which in turn corresponds to the plateau on a pH final vs. pH initial graph. However, that is not always the case. Three key parameters affect the deviation of the PZC form the graph's plateau (5). They are DpK, surface area, and PZC. An increase in DpK or a decrease in surface area leads to an increase in the PZC/plateau deviation (5). However, the most influential factor is the PZC. An extreme (very high or very low) value of the PZC will increase the PZC/plateau deviation (5). Generally, a compound with a PZC outside the range of approximately 3-11 will demonstrate a deviation from the plateau (5). A more detailed explanation of the physical explanations for these deviations may be found in Parks Thesis.

MATERIALS AND METHODS

Several different types of alumina, silica, and carbon were tested in hopes of determining the surface charging parameters' dependence upon the characteristics various substances. The three types tested include a γ-alumina from LaRoche Chemicals with a surface area of 250 m^2/g, α-alumina with a surface area of 101 m^2/g, and a θ-alumina with a surface area of 77 m^2/g. The α-alumina was calcined in a muffle furnace at 500ºC for 3 h. Two types of silica were used. They included fumed silica with a surface area of 90 m^2/g and precipitated silica with a surface area of 300 m^2/g. In addition, several different types of carbon were tested. The activated carbons tested include Norit SX ULTRA 99133 with a surface area of 1200 m^2/g, Norit Darco KB-B that had a surface area of 1500 m^2/g, and Norit CA1 NC99006 with a surface area of 1400 m^2/g. The carbon black used here was CABOT VULCAN XC72 GP-3845, which

had a surface area of 254 m^2/g. Finally, the carbon graphite was Timcal TIMRES HSAG 300 CAT with a surface area of 300 m^2/g.

Sample preparations were not required for alumina and silica, however, in order to clean the ions that were exposed to the surface of the carbon, it was washed before use. Two different methods were used for carbon preparation. First, carbon was combined with deionized water (pH of ~5.8) in an amount greater than ten times its pore volume. The carbon solution was placed in an Eberbach shaker for at least an hour. After that time, the solution was filtered viva suction filtration with a vacuum pump. The moist solid was then dried. For the first set of data, the carbon was placed in a Precision Model 18 oven at 200˚C and allowed to bake overnight. However, the second set of carbon was dried at room temperature (~23˚C) until dry.

One-liter pH solutions ranging from 0 to 13 with increments of approximately 0.5 were prepared using 1N NaOH and HCl attained from Fischer Scientific and deionized water with an initial pH of ~5.8. Due to the instability of slightly basic solutions upon exposure to air, solutions between a pH ~6-11 were allowed to vary (i.e. the increments were sometimes greater/less than 0.5 pH. The ionic strength of the solution was then calculated. NaCl from Fisher Scientific was then added in order to ensure a constant ionic strength of 0.1M. The higher ionic strength also allows the solution to attain more quickly a state of equilibrium without affecting the final pH (7). Unfortunately, the addition of NaCl also increases the rate of CO_2 absorption (7).

The following reactions take place and thereby make the solutions more acidic.

$$CO_2 + H_2O = H_2CO_3$$

$$H_2CO_3 = HCO_3^- + H^+$$

Where necessary, the solution pH was increased with a small NaOH addition. Solution pH was tested at least once daily. Slightly basic solutions, which demonstrate the most notable changes due to CO_2 absorption, were tested immediately before each experiment.

The pH solutions were then combined with various oxides in order to attain a variety of surface loadings. The surface loadings of 500 m^2/L , 6,000 m^2/L, 60,000 m^2/L, and incipient wetness (i.e., maximum oxide content and minimum liquid content) were chosen as representative measurement points. The following equation was used to determine the mass of oxide required:

$$\text{Mass} = (\text{Surface Loading} * \text{Volume of Solutions}) / \text{Surface Area}$$

The oxide was measured and placed in a 60mL Nalgene bottle, 15mL Falcon conical tube or a 12 x 35 mm Fisherbrand glass vial depending on the desired surface loading and solution volume. The pH solution was added to the oxide viva pipet.

After the oxide addition (for all surface loading except incipient wetness), the solution was placed on a shaker for approximately 8 minutes. Final pH readings were recorded with a standard Accumet pH probe approximately 10 minutes after the oxide addition. The probe was calibrated with Thermo Orion pH buffer 4, 7, and10 at least once daily. When the 60mL Nalgene bottles were used, the solution was stirred using magnetic stir bars during the pH measurements. In the case of incipient wetness, the glass vials were utilized. After oxide and solution addition, the vials were tapped vertically on a counter for approximately 8 minutes to ensure proper mixing. The thick nature of the slurry made it necessary to use a spear-tipped pH probe. A special purpose Cole-Parmer probe (catalog number P-05998-20) was used. It was calibrated at least once daily (with pH buffers noted above) and tested periodically to determine whether

recalibration was required. It should be noted that the probe is not reliable at pH >11-12 and has a relatively short life(6).

Previously it was noted that the final pH measurements were taken 10 minutes after the oxide/solution combination. Most oxides reach a state of equilibrium in an electrolyte solution in approximately 10 minutes (5). Unfortunately, in addition to the equilibrium, alumina and silica undergo dissolution, although carbon does not. A general rule for oxide dissolution is that acidic oxides dissolve in basic solutions while basic oxides dissolve in acidic solutions (5). Alumina is amphoteric and its PZC lies at a central pH value, so it may become acidic or basic.(1) Thus, it undergoes dissolution at pH values <4 and >10. Silica is also amphoteric, but its PZC is located in the acidic range(1). Since only a negligible amount of positively charged sites exist below the PZC, silica could be classified at a single site oxide (1). In other words, silica is primarily an acidic oxide, and thus, it dissolves in basic solutions.

The following example of what is thought to occur in the dissolution of silica (3):

1. Molecular water diffuses into silica.
2. There is a reaction with the silicon-oxygen lattice.
3. Silica polymers are formed.
4. Polymers are broken down to monomeric silicic acid by hydrolysis.

Overall, the following reaction takes place:

$$2H_2O + SiO_2 = H_4SiO_4 \text{ (monomer)}$$

Then, in basic solution the monomer undergoes the following reaction:

$$H_4SiO_4 = H^+ + H_3SiO_4^-$$

A contact time of 10 minutes was chosen in hopes of ensuring that equilibrium was reached while minimizing the time allowed for oxide dissolution. Several experiments were conducted to determine more precisely the kinetics of the reaction. The following graphs show that when the pH solutions were outside the dissolution range for silica and alumina, equilibrium was reached after roughly 10 minutes of oxide contact time.

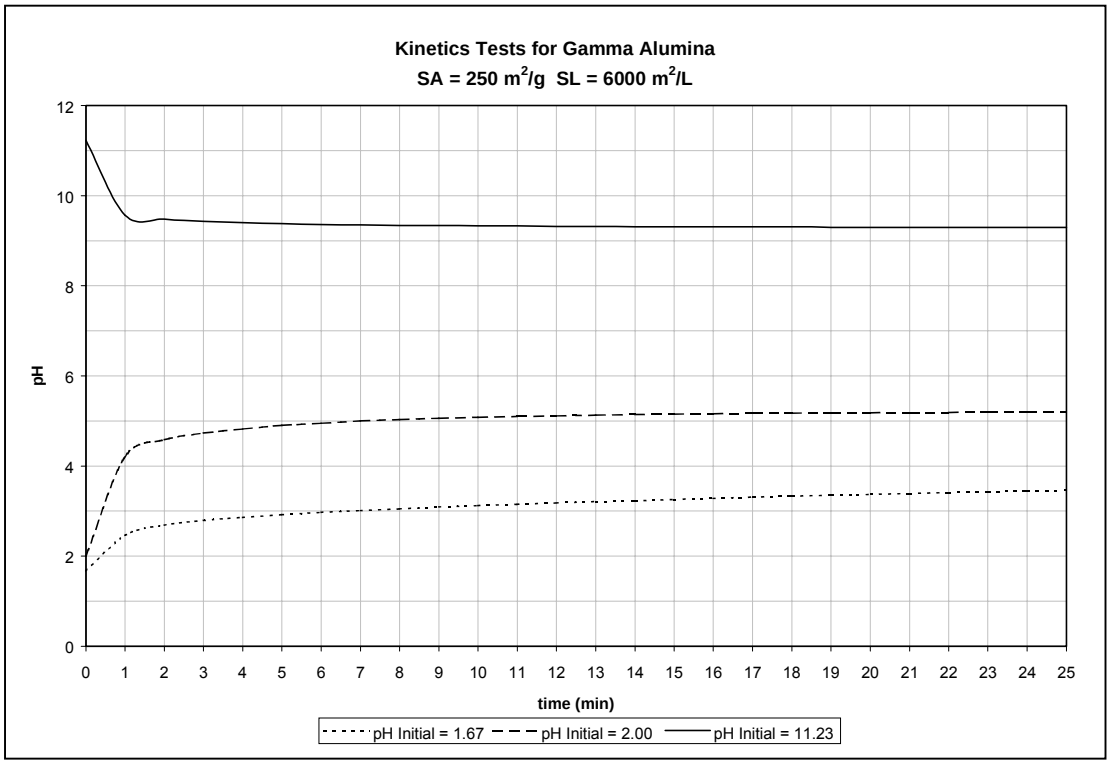

Figure 4. A graphical representation of the kinetics involved with gamma alumina.

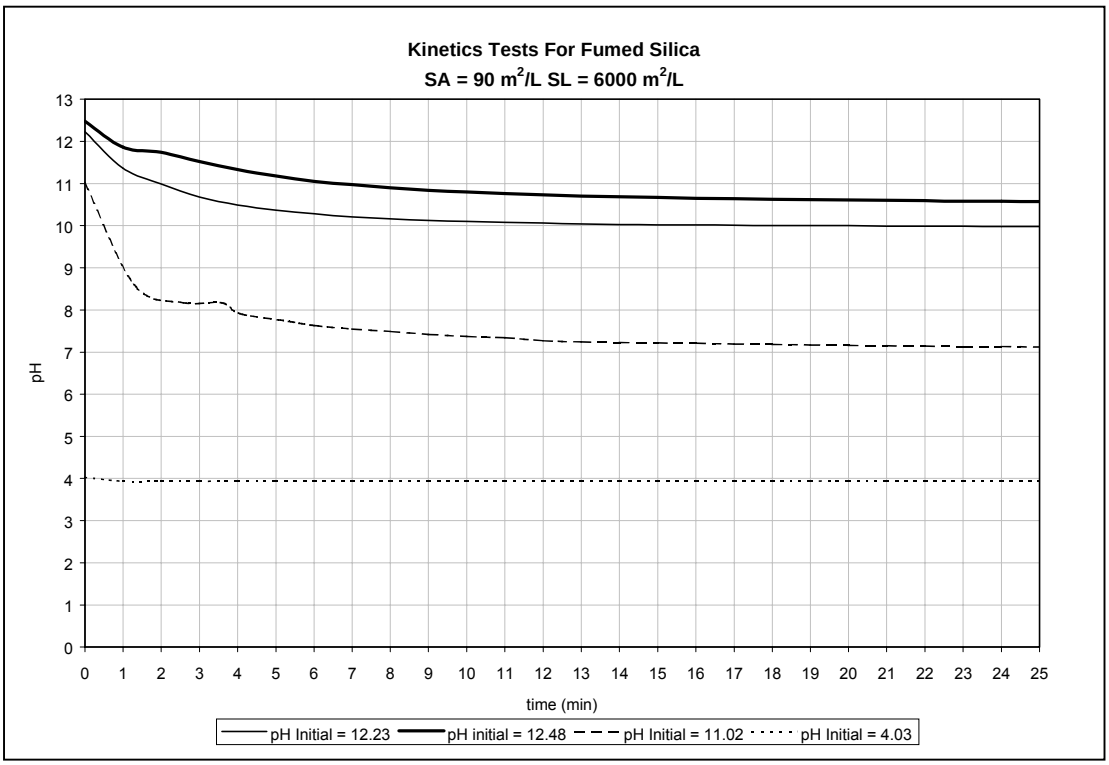

Figure 5. A graphical representation of the kinetics involved with fumed silica.

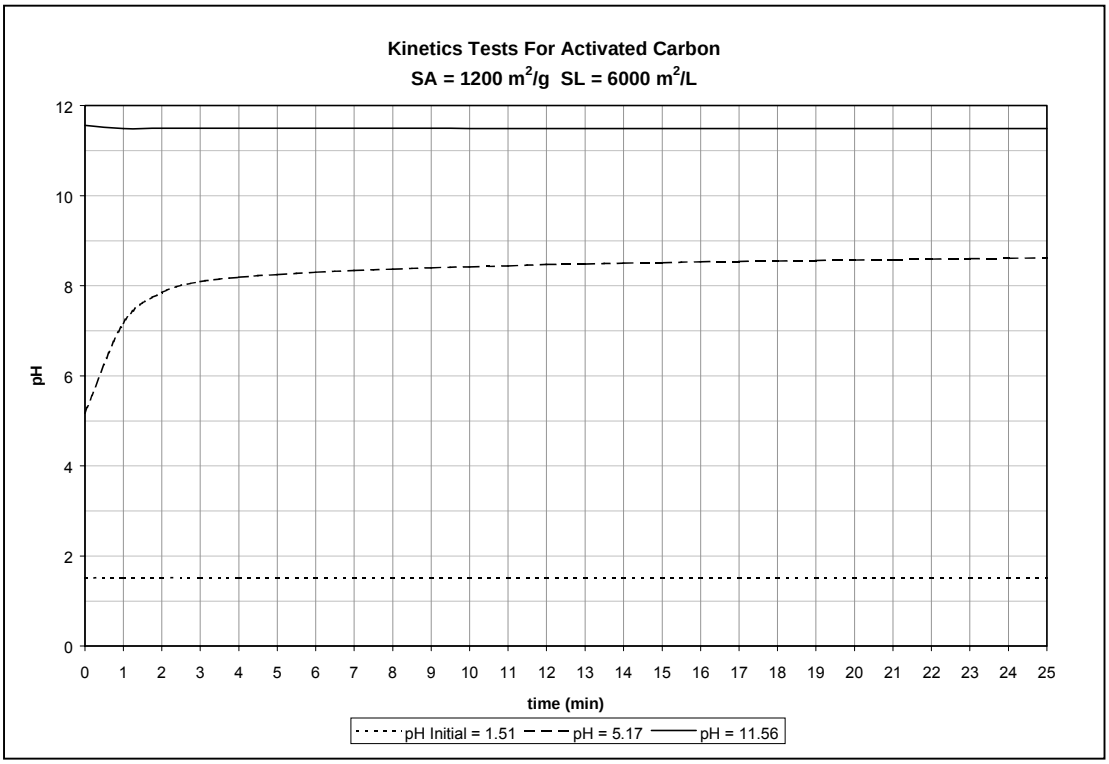

Figure 6. A graphical representation of the kinetics involved with Activated Carbon.

Initial experiments for carbon were allowed a contact time of 10 minutes. However, strange instability was noticed in a pH range of approximately 3.5-11. The graph here demonstrates that the pH values are very stable in extremely acidic and basic conditions. However, the middle pH value exhibits a gradual, continual change. Due to this experiment, a contact time of 30 minutes was allowed for later experiments with initial pH in before mentioned range.

RESULTS AND DISCUSSION

Massive data was collected. This data was fitted with values obtained from the RPA model. Recall that three equations were simultaneously solved to determine the values for Γ_o, σ_o, and H_f. In order to do this, the values for the three other unknowns (PZC, DpK, and Ns) were altered until the data and the model agreed. This, of course, is not the optimal approach. In the future, an optimization model should be formulated to determine the precise values of these parameters. The current data values are supported by various sensitivity analyses that demonstrate the effect of changing one parameter while holding all others constant. The purpose here is to show that the current values are at least reasonably accurate and to demonstrate which part of the graph is affected by changing each parameter. The Ns sensitivity graphs seen below show that varying Ns leads to changes in the "tails" of the graph. While the DpK sensitivity demonstrates that altering the value of DpK changes the width of the PZC plateau. Notice that PZC variation was not graphed. Changing the PZC only alters the location of the plateau. This is not necessary since our data demonstrates fairly well exactly where the plateau is located.

Ns Sensitivity

After a literature study was done the next step was to visually see the dependence of the s value on the RPA Model. For every material that was modeled a Surface Loading of 6000 m^2/L was used. In each case a pzc and DpK value was chosen that best fit the experimental data using, in the case of alumina and silica, the most commonly used literature value being 8 and 4 sites/nm^2 and for carbon the best fit value of Ns was used due to the lack of literature values found. After each pzc and DpK were found for the respective Ns values, the pzc and DpK were held constant while the Ns values were varied by the magnitudes shown on each graph. As can be seen, although the change in Ns in each plot differs, there is a definite effect to the model

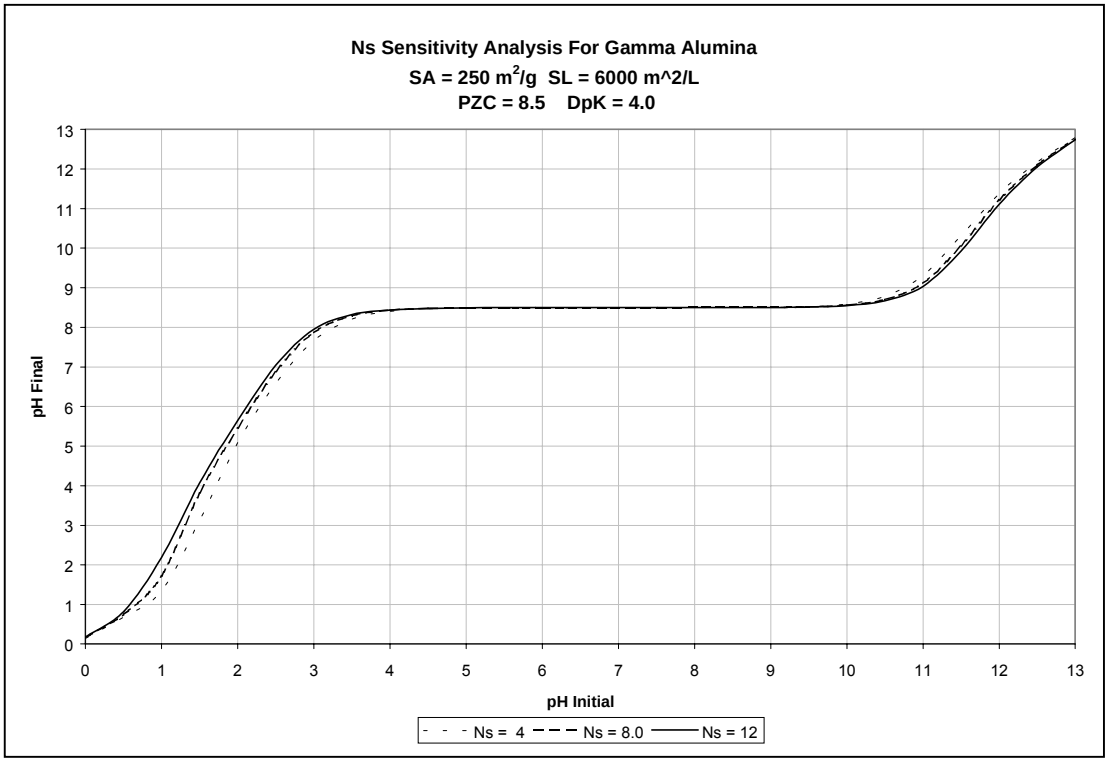

Figure 7. A graphical representation of the sensitivity of Ns for Gamma Alumina.

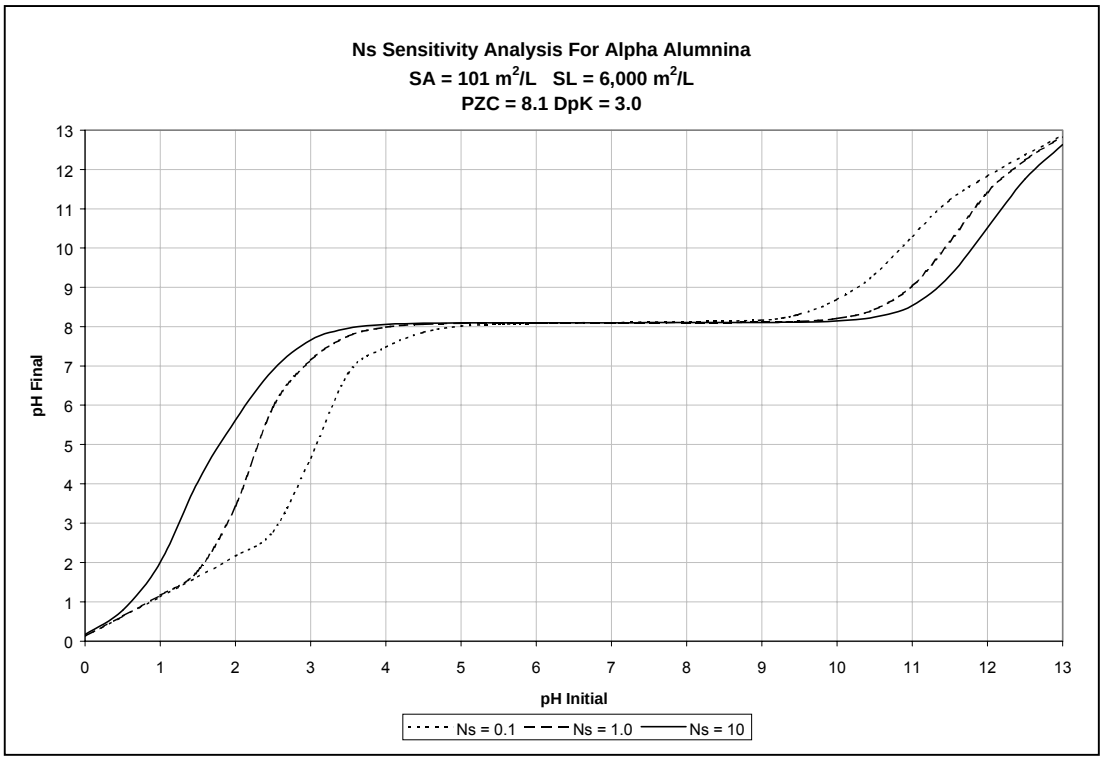

Figure 8. A graphical representation of the sensitivity of Ns for alpha alumina.

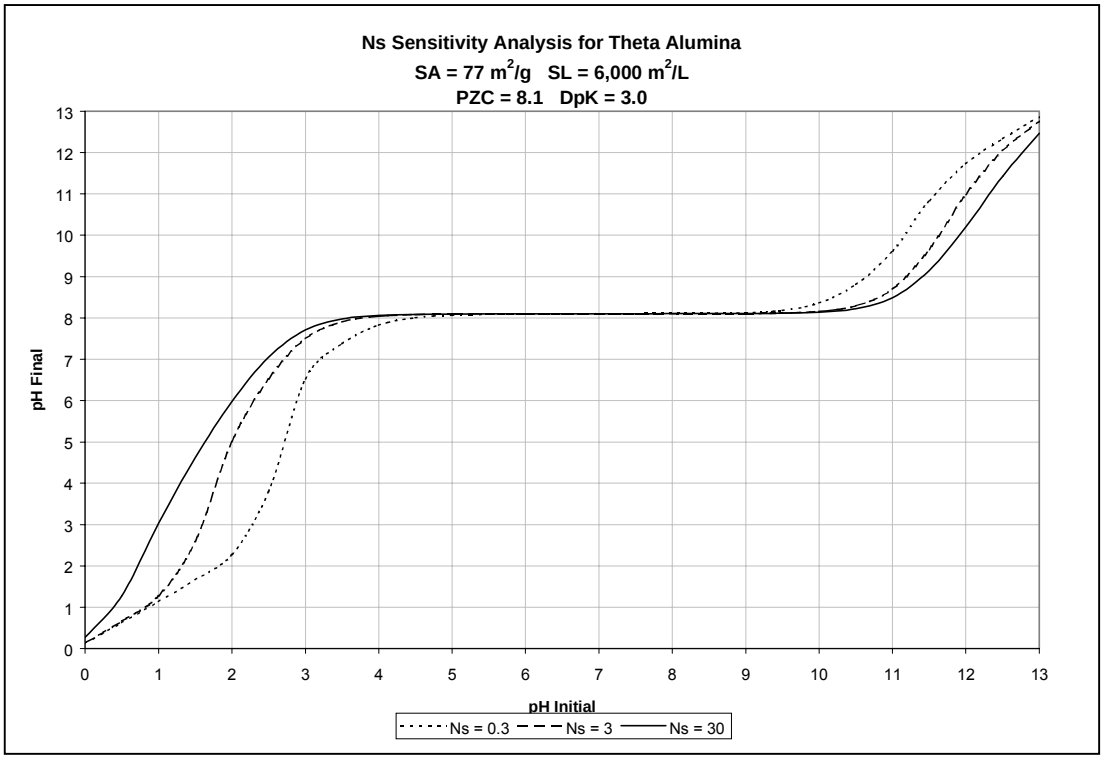

Figure 9. A graphical representation of the sensitivity of Ns for theta alumina

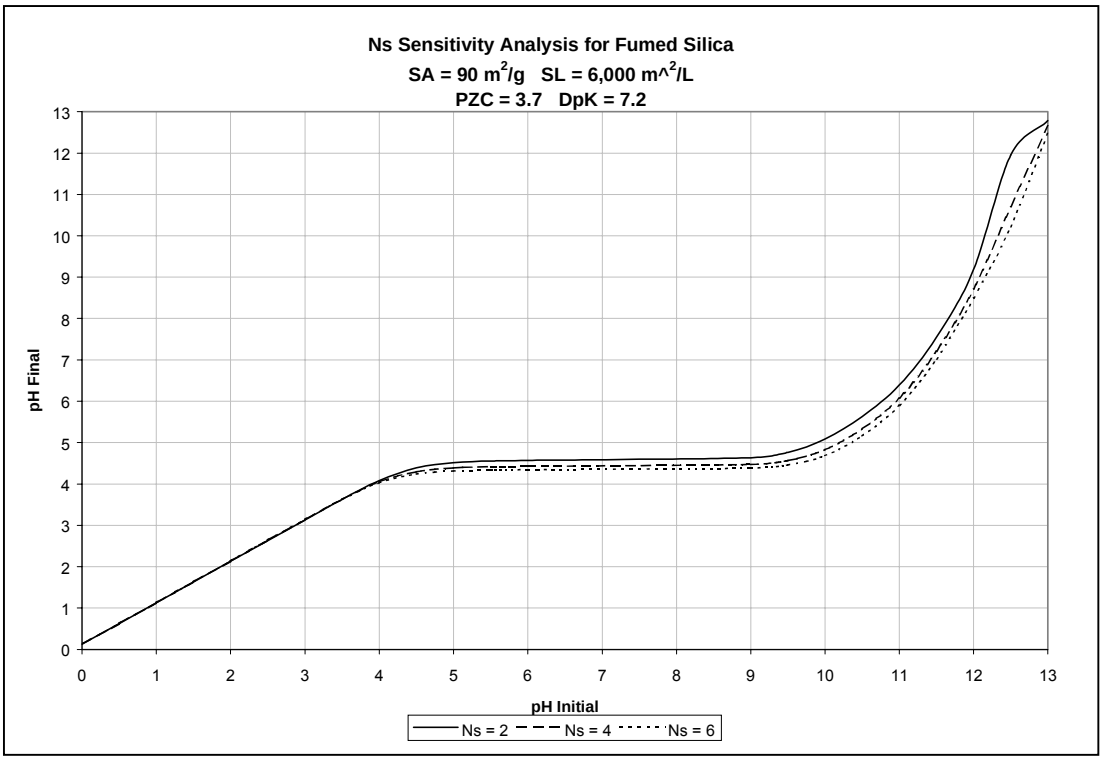

Figure 10. A graphical representation of the sensitivity of Ns for fumed silica

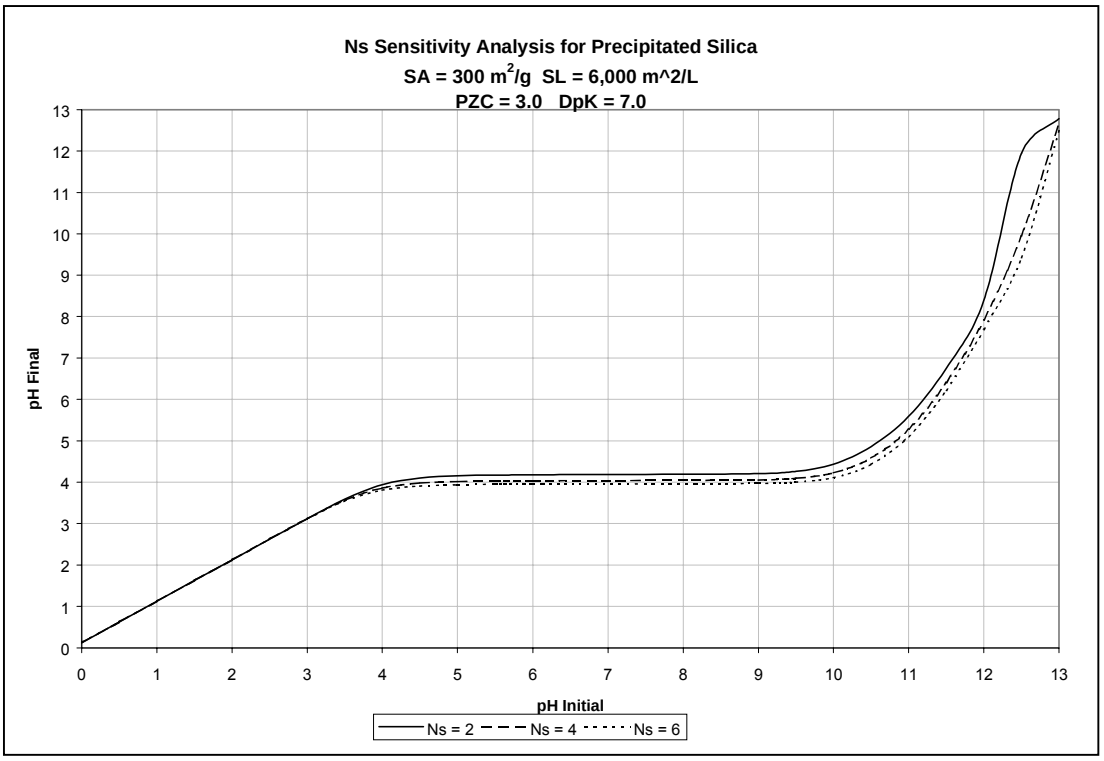

Figure 11. A graphical representation of the sensitivity of Ns for precipitated silica

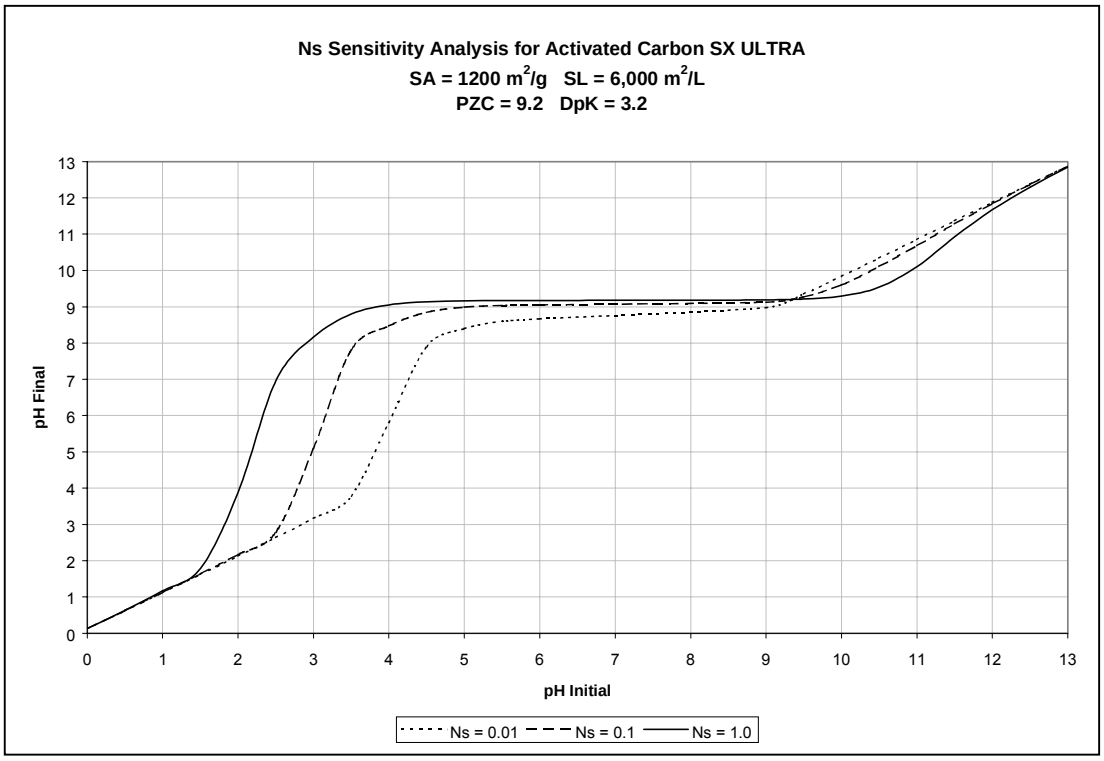

Figure 12. A graphical representation of the sensitivity of Ns for activated carbon.

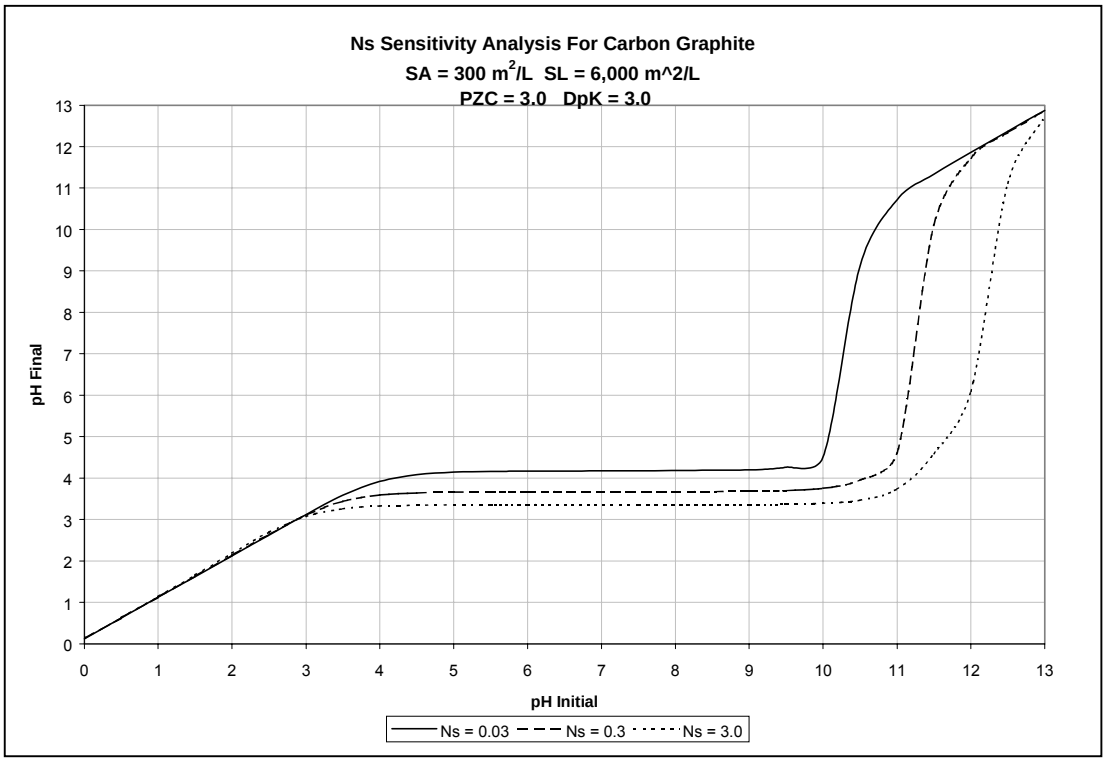

Figure 13. A graphical representation of the sensitivity of Ns for carbon graphite.

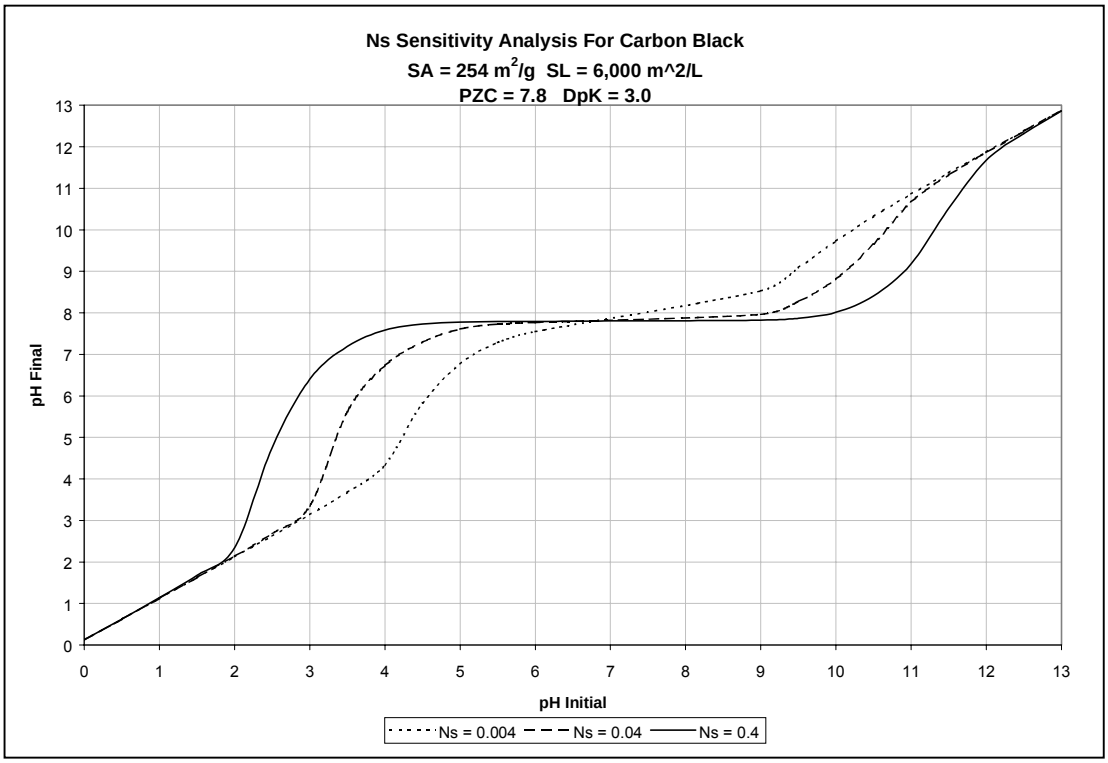

Figure 14. A graphical representation of the sensitivity of Ns for carbon black.

DpK

In an ex tended sensitivity analysis studies of the effects of the DpK on the model were plotted. In a hope to make more sense of the Ns value, the DpK value was varied to see if it would cause the same change in the model. For the aluminas and silicas, again, the literature Ns values of 8 and 4 sites/nm^2 were used and the best-fit pzc was applied to the plot. As noted previously, due to the lack of literature found at the time the best fit values for the Ns and the pzc for all the carbons were employed. This time the DpK values were varied, as seen, and the Ns and pzc ere held constant. When these plots are compared to those created with the Ns sensitivity analysis, it can be seen that the Ns values effect the curvature of the model in different ways than the DpK value does. The study thus far is inconclusive, but as soon an optimization program is done and an even

greater literature review is done then a more conclusive result can be drawn on why these variations occur.

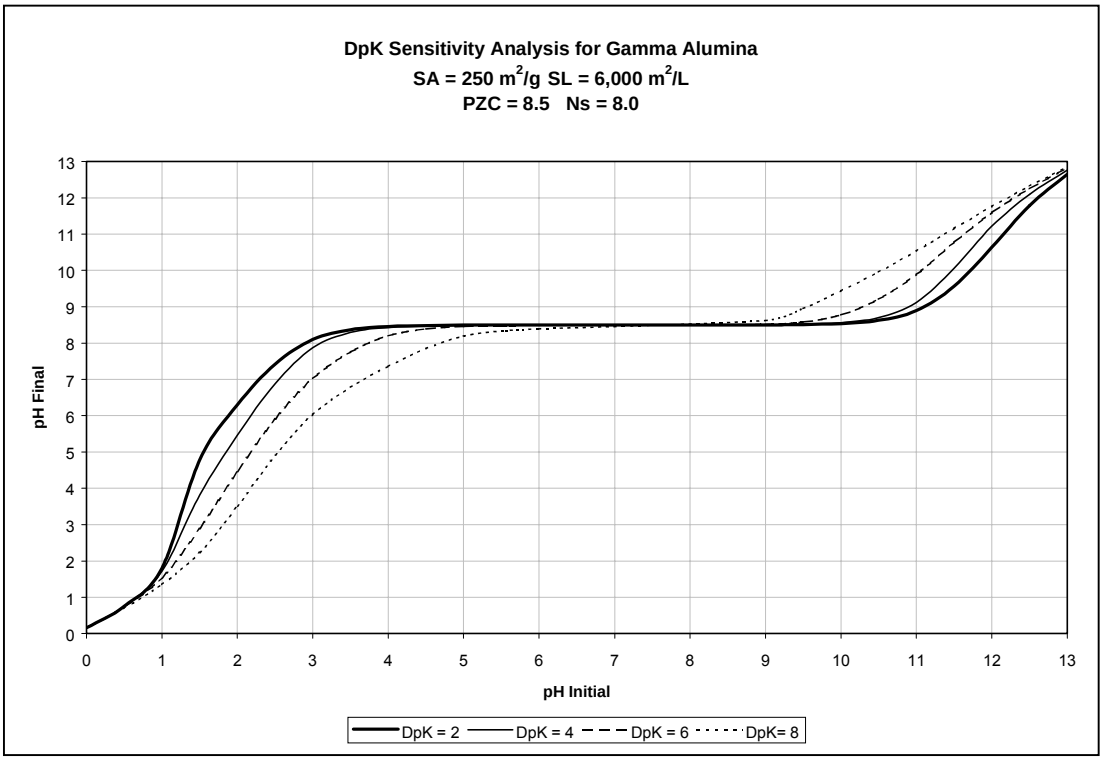

Figure 15. A graphical representation of the sensitivity of DpK for gamma alumina.

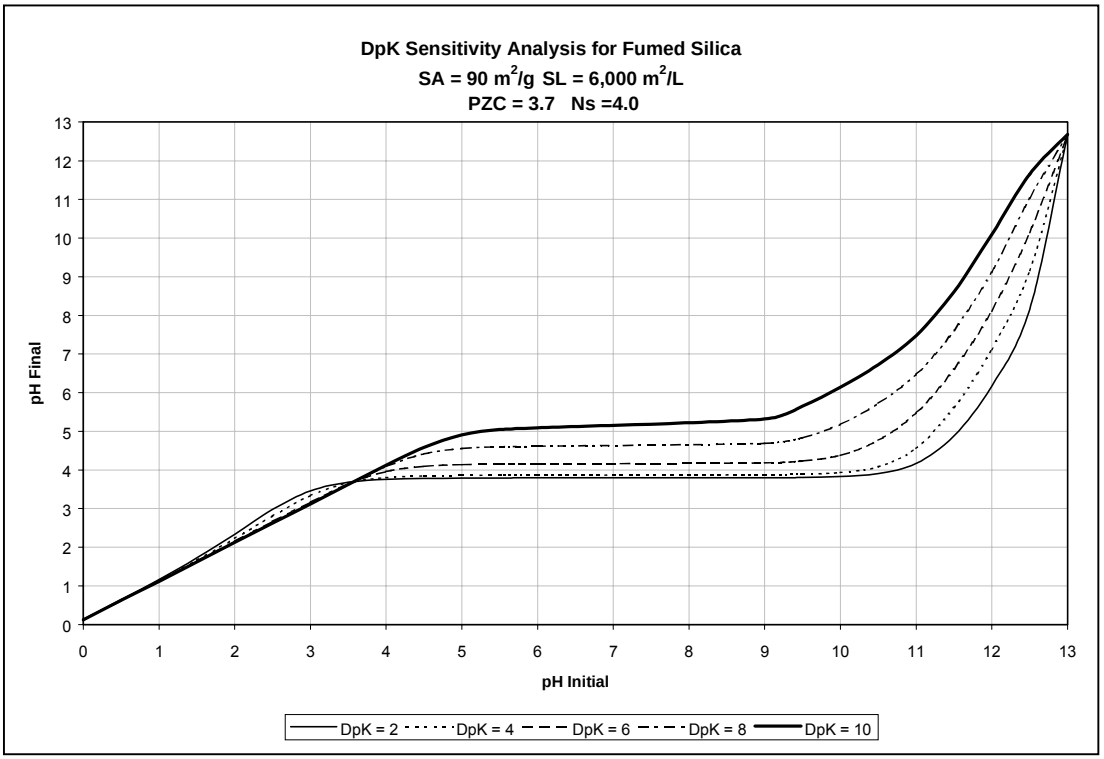

Figure 16. A graphical representation of the sensitivity of DpK for fumed silica.

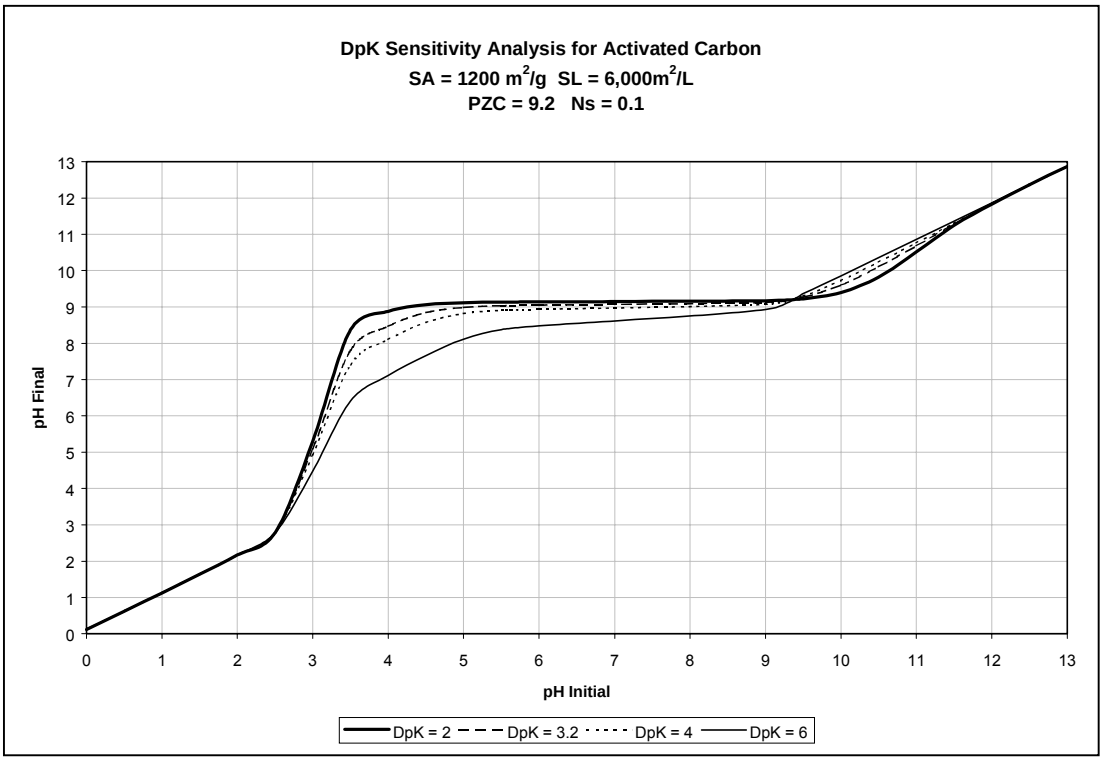

Figure 17. A graphical representation of the sensitivity of DpK for activated carbon.

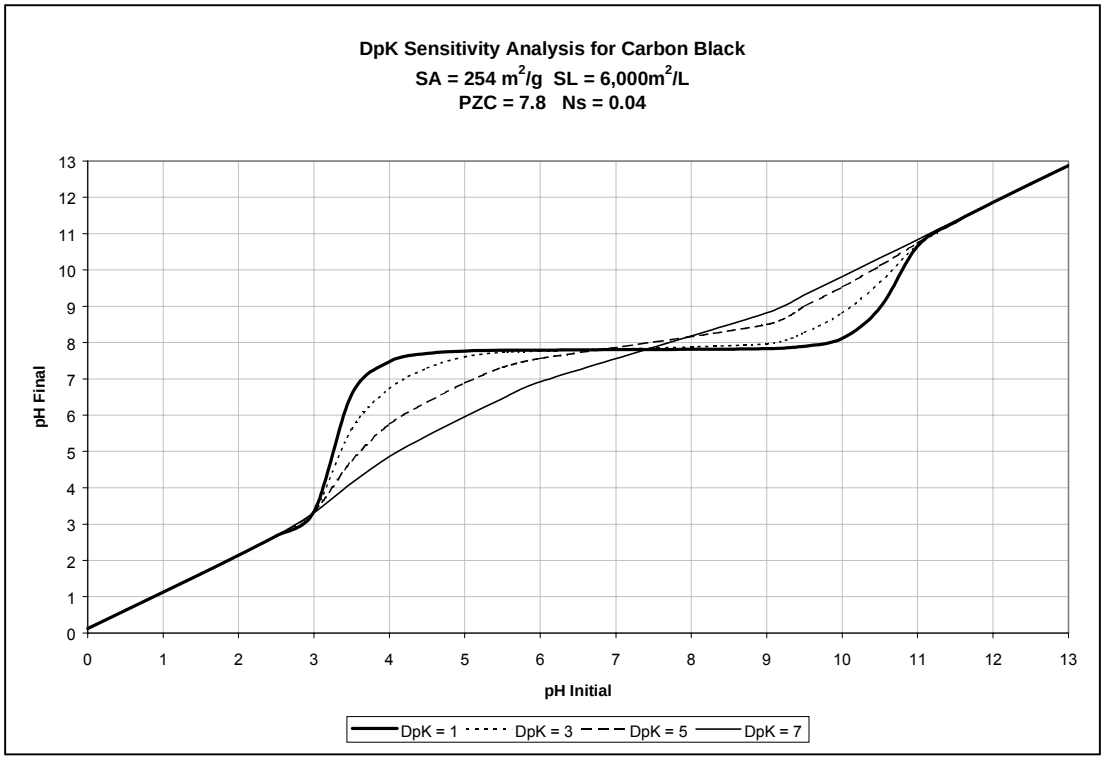

Figure 18. A graphical representation of the sensitivity of DpK for carbon black.

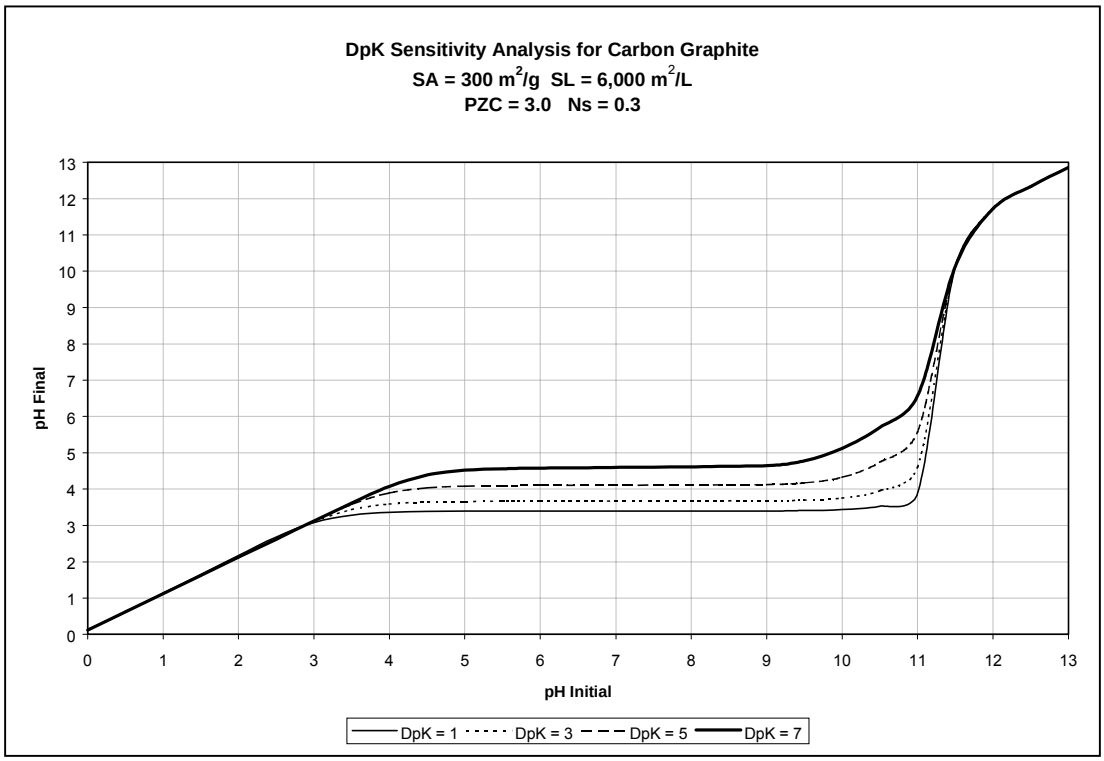

Figure 19. A graphical representation of the sensitivity of DpK for carbon graphite.

Alumina

Experiments were performed on three different types of alumina: gamma, theta, and alpha. Gamma alumina, surface area of 250 m^2/g, was tested at four different surface loading ranging from 500 m^2/L to incipient wetness. Due to lack of material, theta alumina, surface area of 77 m^2/g, and alpha alumina, surface area of 101 m^2/g, could only be performed at a surface loading of 6,000 m^2/L. As noted before an optimization program could not be used, so for now varying the PZC, DpK, and Ns had to be done and a visual determination was used to find the best-fit model. Also, the Ns literature values, documented previously, for gamma alumina were found to be around 8

OH/nm^2, but it was found, Figure 3, that an Ns value equal to 2 OH/nm^2 along with a PZC of 8.5 and a DpK value of 2.0 visually fit the experimental data.

As for alpha and theta alumnia, thus far, there have not been any documented values found for Ns. In an attempt to keep the PZC and DpK the same for both theta and alpha alumina and just vary the Ns value, the model, seen in Figure 21, accurately fit both aluminas with a PZC of 8.1, a DpK of 3.0, an Ns for alpha alumina of 1 OH/nm^2, and an Ns value of 3 OH/nm^2.

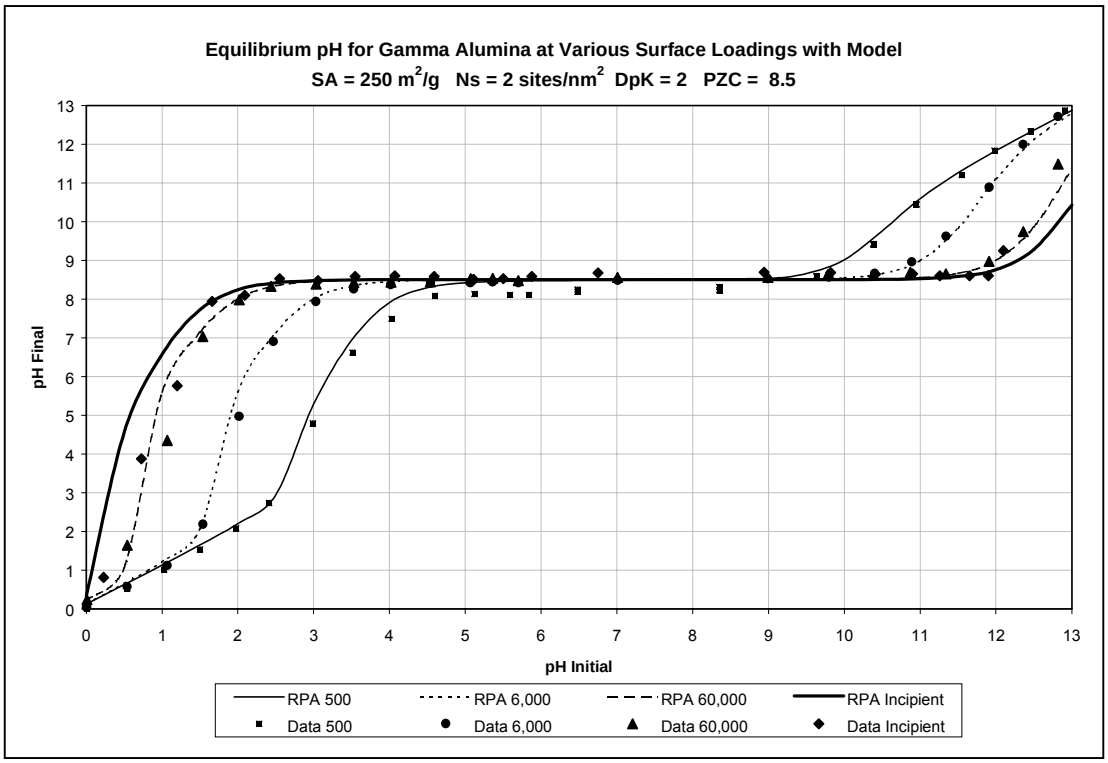

Figure 20. A graphical representation the pH shift of gamma alumina at various surface loadings.

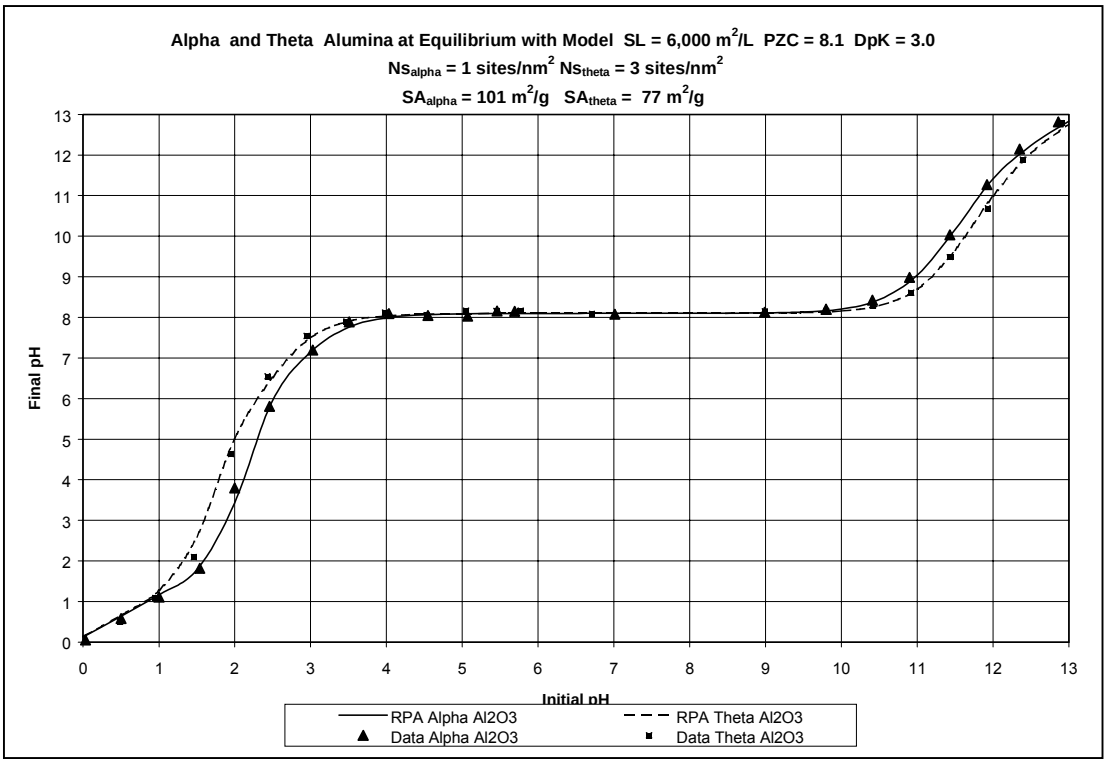

Figure 21. A graphical representation the pH shift of alpha and theta alumina at a surface loading of 6000m^2/g.

Silica

Experiments were also performed on two different types of silica: fumed silica, with a surface area of 90 m^2/g, and precipitated silica, with a surface area of 300 m^2/g. Each were tested at three different surface loadings (m^2/L): 500, 6000, and incipient wetness. The Ns values found in Figure 3, varied but seem to average around 4 to 5 for both types of silica. It was found through visual analysis the model seemed to fit the experimental data for precipitated silica, Figure 21, Ns = 0.9 sites/nm^2, DpK = 7.0, pzc = 7.0 and for fumed silica, Figure 22, Ns = 1.5 sites/nm^2, DpK = 7.5, pzc = 3.0.

As one can see from the figures, there are a lot of out lying points in the basic range. More than likely, this has to do with the dissolution of silica that was explained in

previous section. Hopefully, when an optimization program is produced the model will more accurately fit the data in these figures.

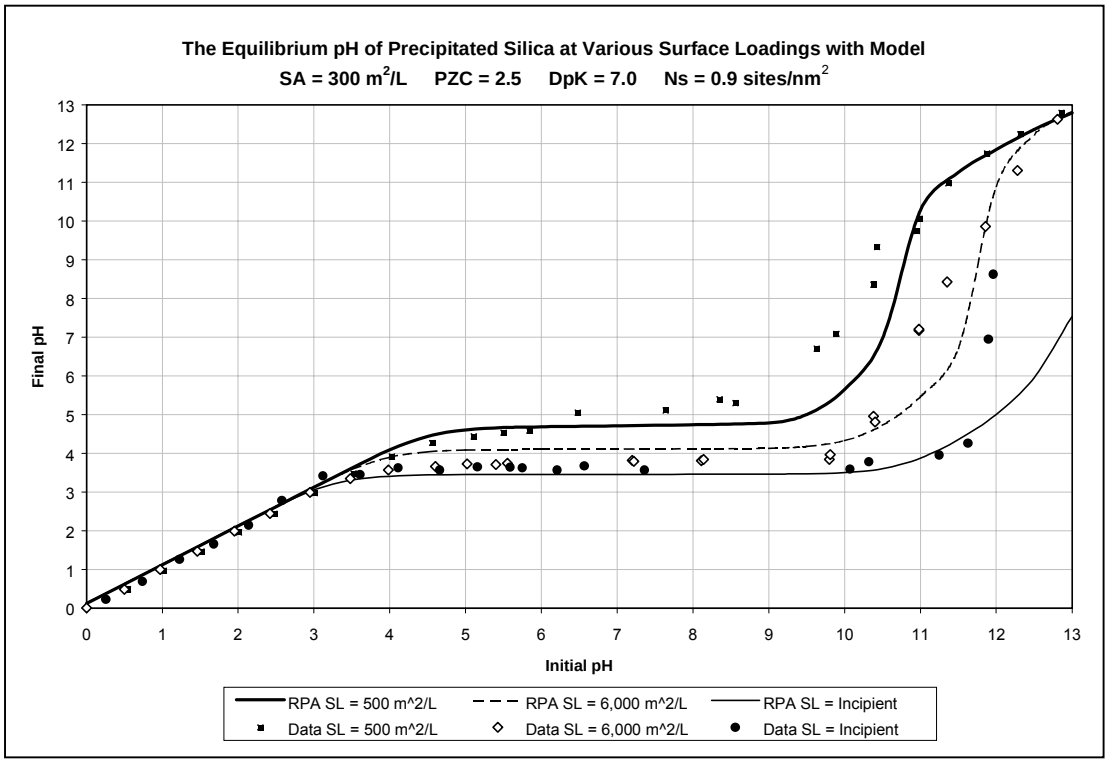

Figure 22. A graphical representation the pH shift of precipitated silica at various surface loadings.

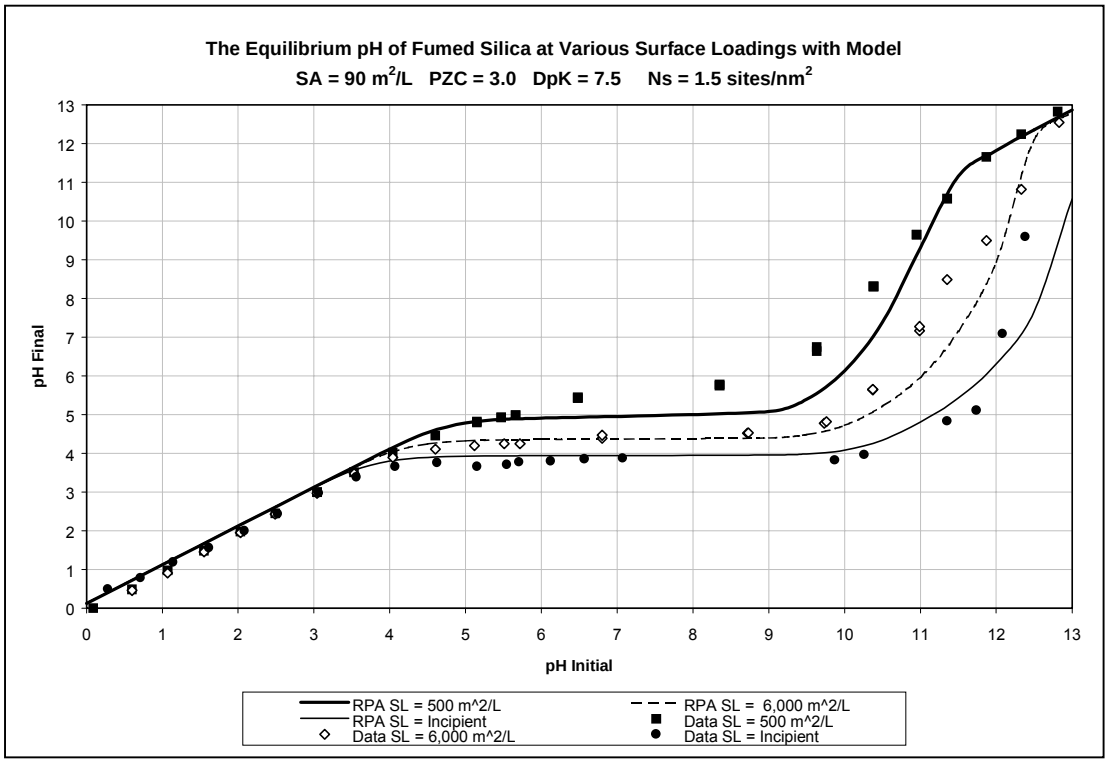

Figure 23. A graphical representation the pH shift of fumed silica at various surface loadings.

Carbon

Three different types of carbon were tested and modeled at various surface loadings. The results from the RPA model may be seen on the graphs below. As noted above, there were no literature values found thus far for the Ns values for the carbons used.

As noted previously, two different techniques of drying were used. The carbons in Figures 23, 24, and 25 were dried in the oven at 200˚C, while the carbons in Figures 27, and 28 were dried at room temperature. Figure 26 demonstrates the different drying techniques lead to a shift in the PZC. The current hypothesis is that the oven drying promotes the destruction of carboxylic acid groups that are thought to be located on carbon's surface. It is also important to note that the carbons in Figures 23, 24, 25, and 26 were tested after a contact time of 10 minutes because the instability of carbon's middle pH range was not discovered until after these experiments were completed. Figures 27 and 28 both depict carbon results where the middle pH range was tested after a contact time of more than 30 minutes.

Note that due to time constants, the RPA Model has not been fitted to the carbon data in Figures 26, 27, and 28.

Carbon is more complicated than alumina and silica. Rather than simply possessing hydroxyl groups on surface, it is thought to contain several other groups including carboxylic acid, ketone, etc. Due to this complication, it is believed that a two site model will better fit the carbon data and make more physical sense. For example,

currently, the Ns values attained for carbon seem to be too small. It is hypothesized that a two-site model will lead to more reasonable Ns values.

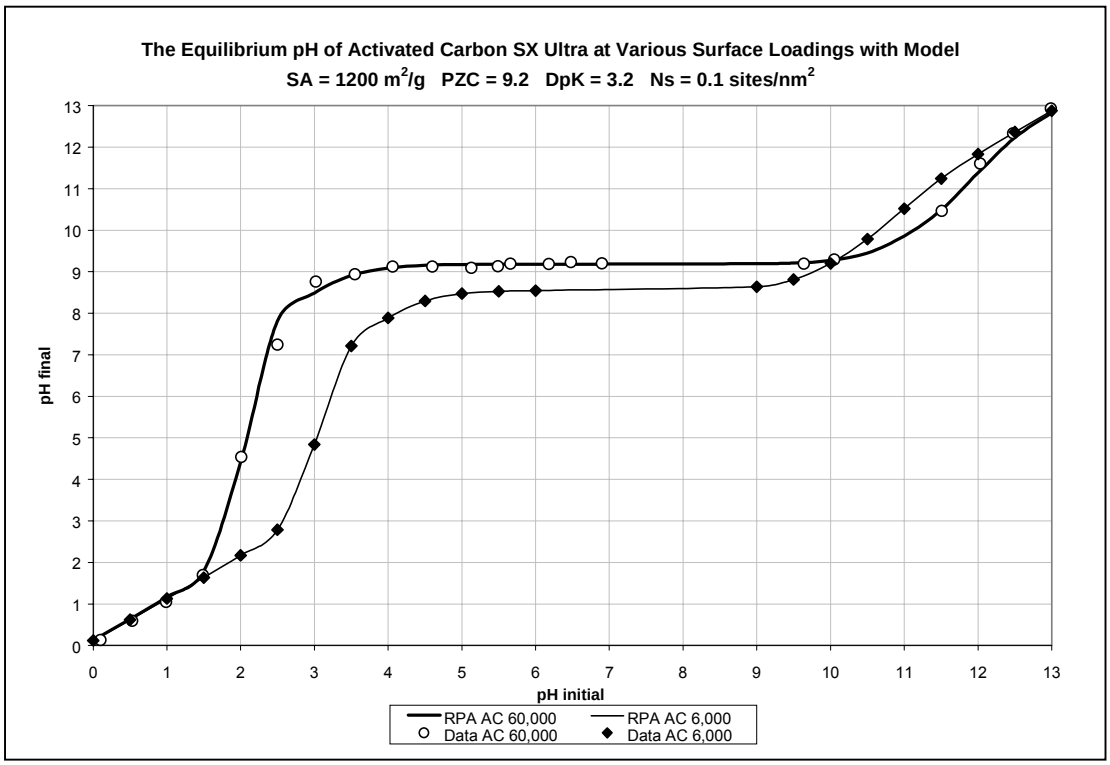

Figure 24. A graphical representation of the pH shift of activated carbon at various surface loadings. It should be noted that the carbon was oven dried and the readings in the middle pH range were taken after 10 minutes, not 30 minutes. So, they may contain some inaccuracy.

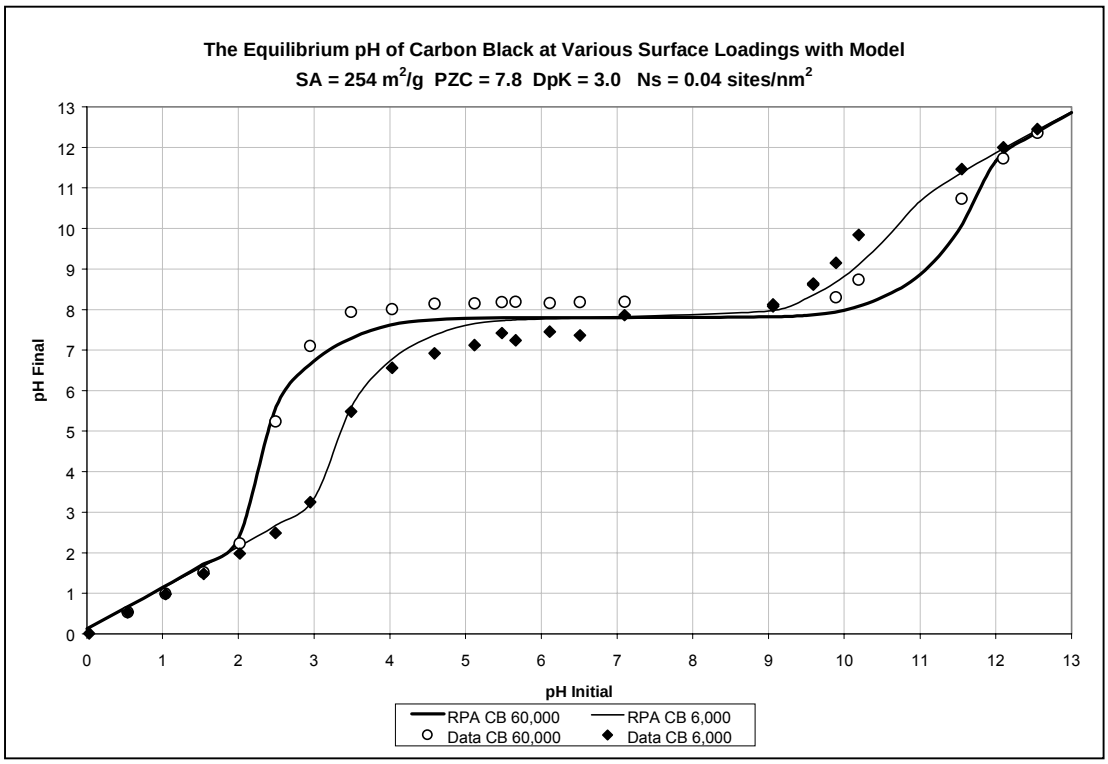

Figure 25. A graphical representation of the pH shift of carbon black at various surface loadings. It should be noted that the carbon was oven dried and the readings in the middle pH range were taken after 10 minutes, not 30 minutes. So, they may contain some inaccuracy.

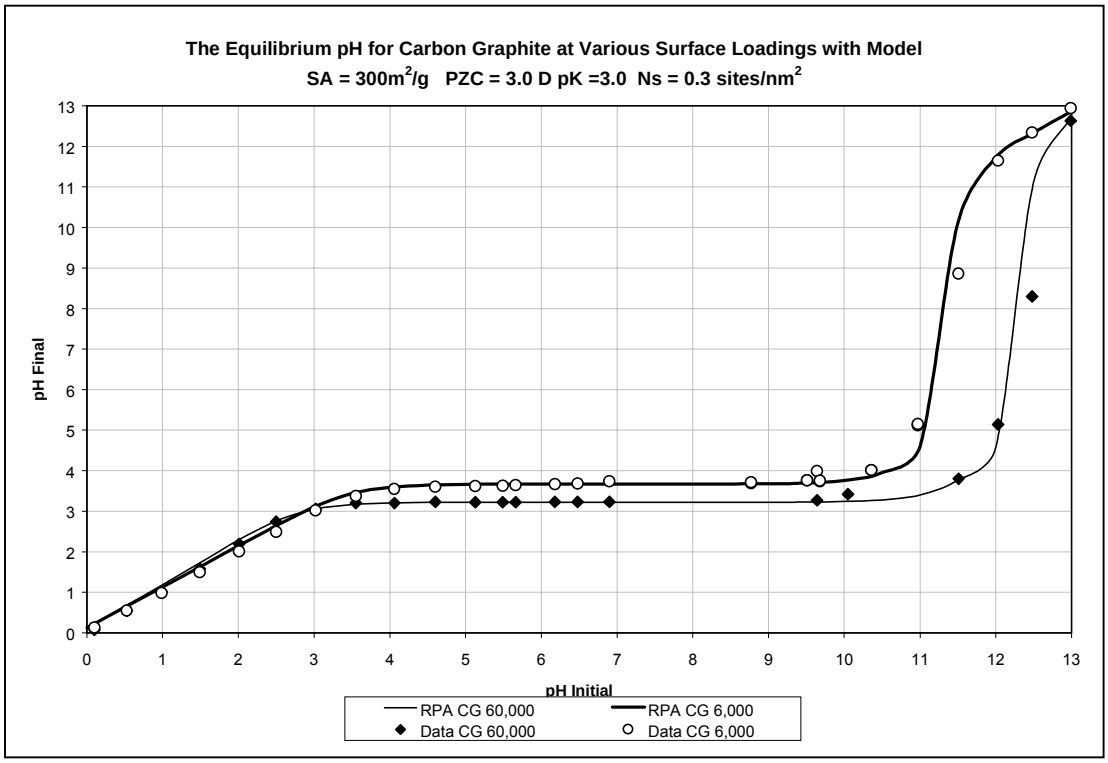

Figure 26. A graphical representation of the pH shift of carbon graphite at various surface loadings. It should be noted that the carbon was oven dried and the readings in the middle pH range were taken after 10 minutes, not 30 minutes. So, they may contain some inaccuracy.

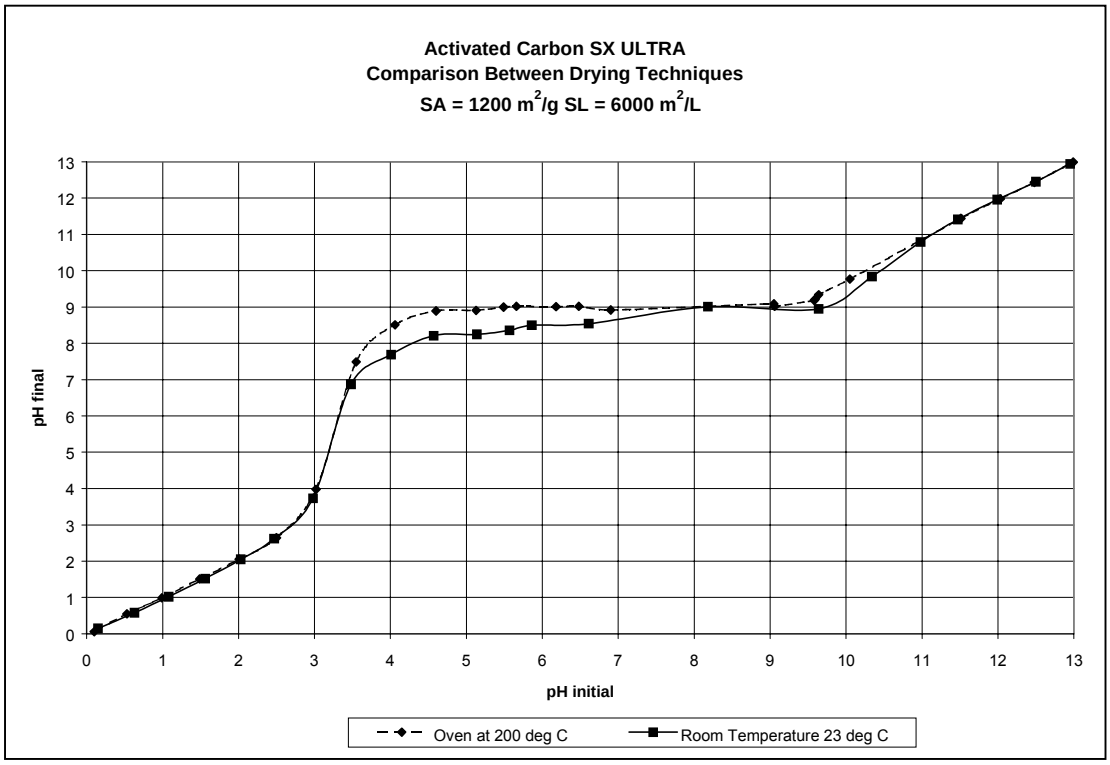

Figure 27. A graphical representation the pH shift of activated carbon at a surface loading of 6000m^2/L. This is a comparison between carbon dried at room temperature and carbon dried in an oven. Data in the middle pH range were taken after 10 minutes, not 30 minutes. So, they may contain some inaccuracy.

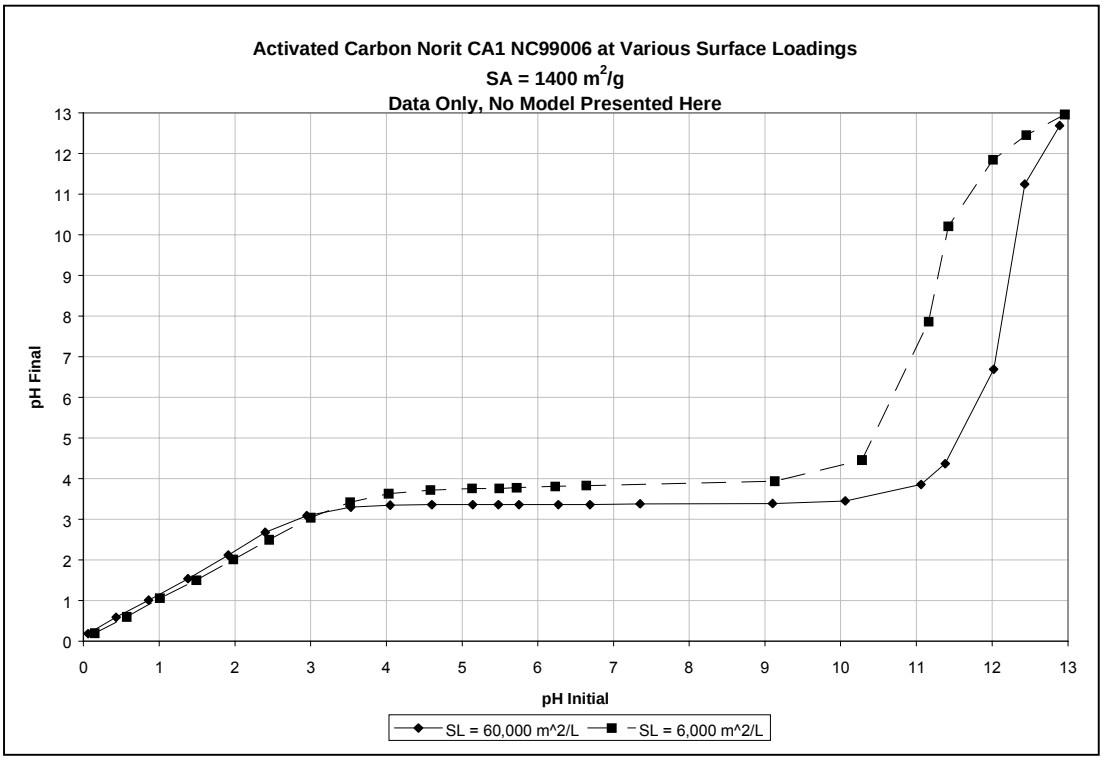

Figure 28. A graphical representation the pH shift of activated carbon at various surface loadings. Here carbon was dried at room temperature and the data in the middle pH range were taken after 30 minutes.

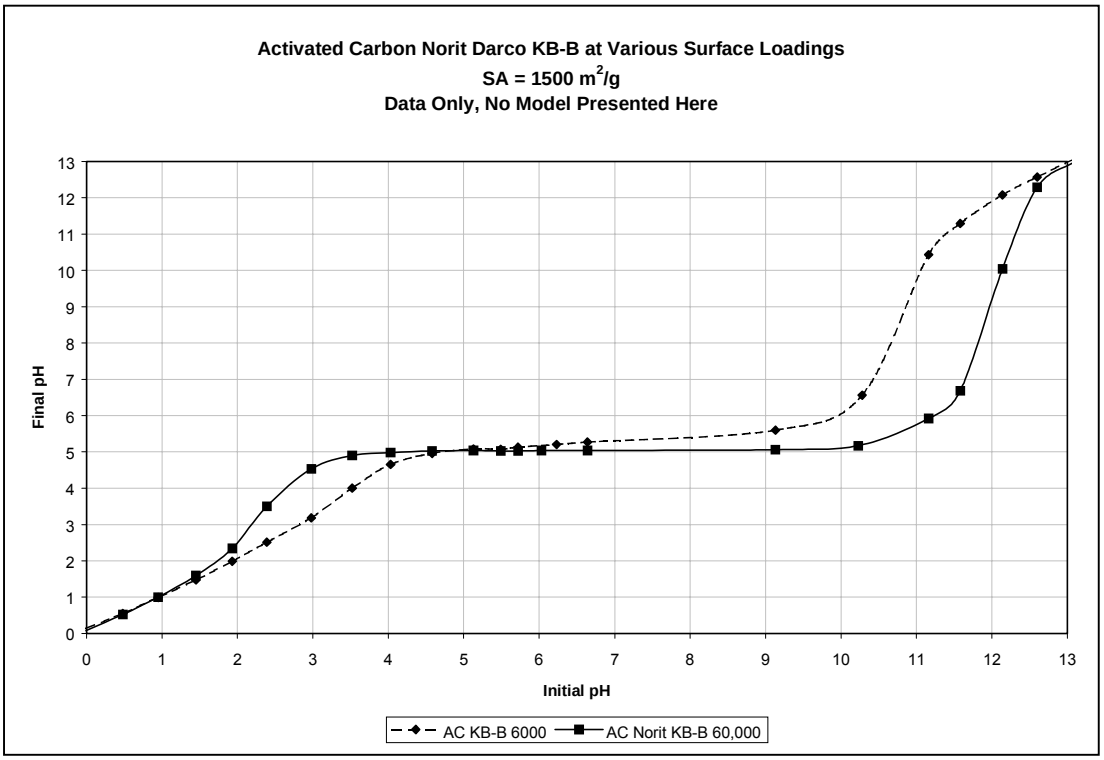

Figure 29. A graphical representation the pH shift of activated carbon at various surface loadings. Here carbon was dried at room temperature and the data in the middle pH range were taken after 30 minutes.

DATA REPRODUCIBILITY

In order provide evidence that our experimental data and our analytically derived model is accurate the following two tests were performed and the plots shown in Figures 29 and 30. First, for our experimental results we tested γ-alumina, SA = 250 m^2/g, at a SL of 6000 m^2/L. Two tests were performed one week apart and the probe was calibrated before each run. Second, for our analytical model which was produced using the program MathCAD, we modeled γ-alumina, SA = 250 m^2/g, at a SL of 6000 m^2/L, pzc = 8.5, DpK = 2, Ns = 2. The data was compared the one created by graduate student Xhainghong Hao using the program Maple. Since the results produced by each were so precise, one is shown with a line and the other with points. The accuracy in both of these plots shows that both our experimental method and model were sufficient.

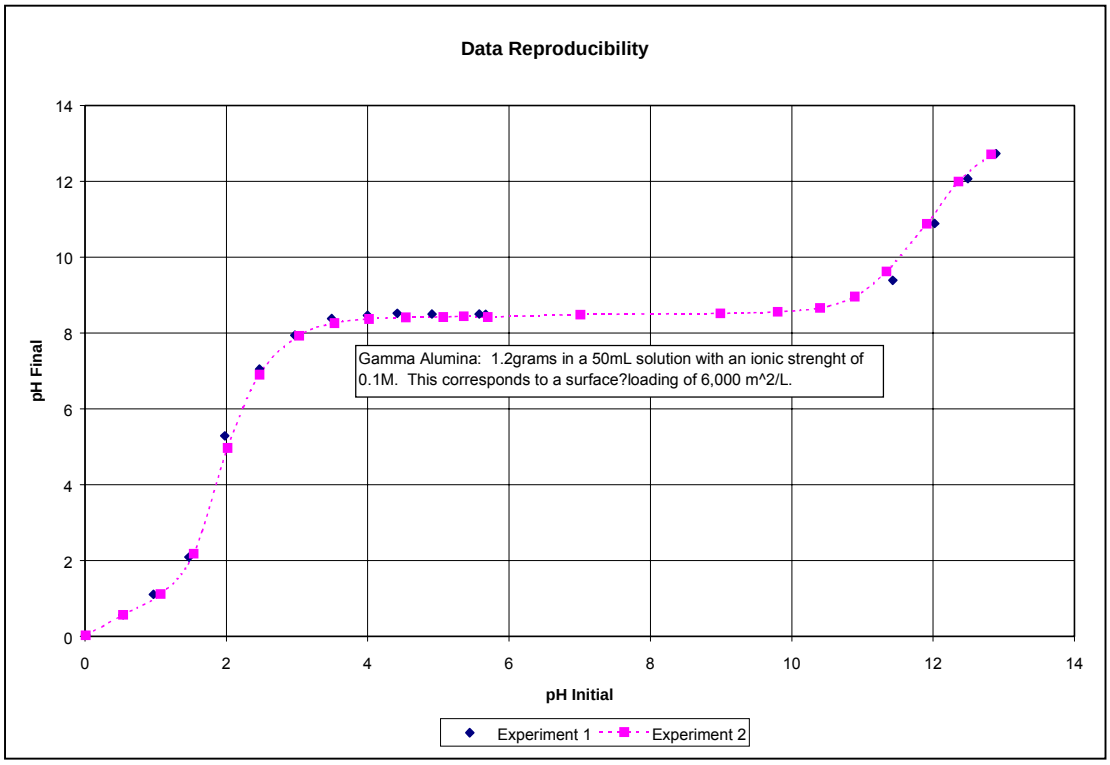

Figure 30. This is a graphical representation of the data reproducibility attained.

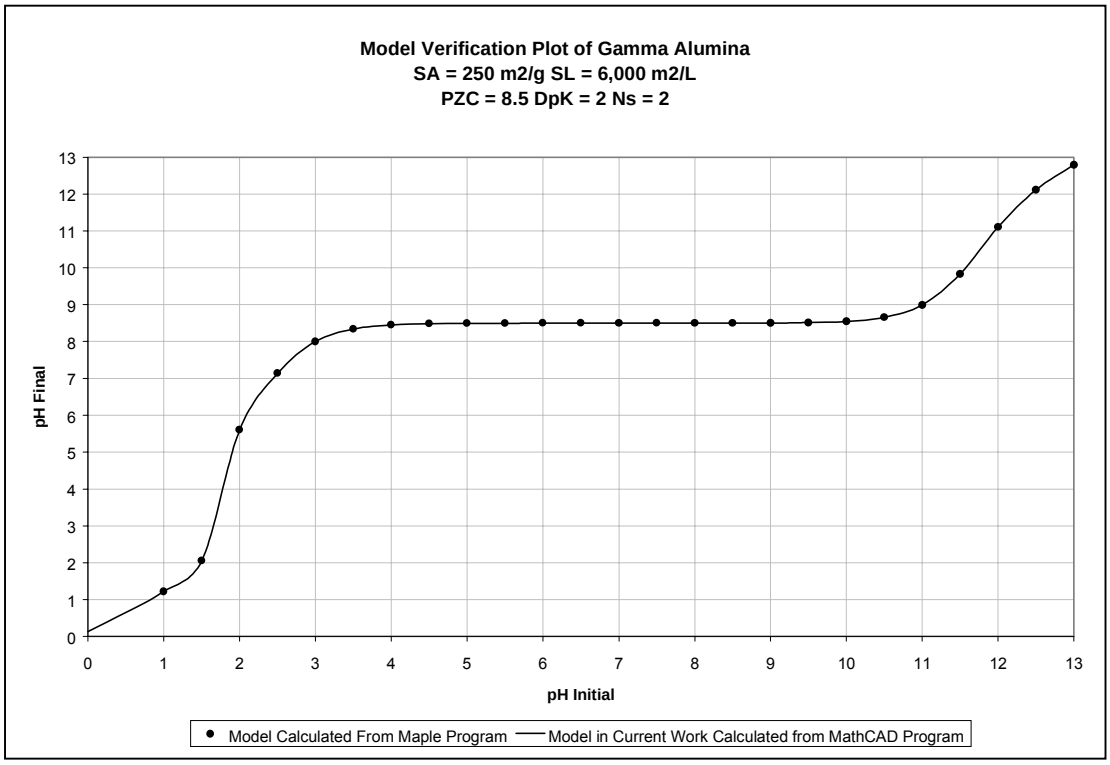

Figure 31. This is a graphical representation of the compatibility of the Maple and MathCAD RPA models.

CONCLUSION

For the benefit of future researchers, the following problems were encountered and should be taken into account before beginning experimentation. First, the spear tipped pH probe is extremely inaccurate within a high pH range. Some method should be developed to account for this error. In addition, carbon dioxide absorption increases with increasing ionic strength (7). Those solutions within an initial pH range of ~7-11 should be tested regularly.

The PZC values attained from this method seem to correspond fairly well with values found in literature. However, the Ns values attained do not agree with literature values. It should again be noted that Ns values found in literature vary greatly. From the current research it is hypothesized that Ns values vary depending on the method of preparation, the oxide surface area, and the exact type of oxide used. Overall, the simple experimental method used here appears to accurately predict the solution pH shift. Of course, the attained values could be improved upon through an optimization program.

ACKNOLAGEMENTS

For giving us the opportunity and for immense value of this experience we would like to strongly thank the National Science Foundation, the University of Illinois at Chicago, the head organizers of the REU Program Dr. C.G. Takoudis and Dr. A.A Linninger, Dr. Kenneth Brezinski the Chemical Engineering Department Head, our inspirational advisor Dr. J.R. Regalbuto, and the hard working graduate students, Xhainghong Hao, Jianming Liu, and Marc Schreier for their tremendous help.

REFERENCES

1. Agashe, Kirshna, *A Revised Physical Adsorption Model for Catalyst Impregnation*,
2. Agashe, Kirshna and John Regalbuto, *A Revised Physical Theory for Adsorption of Metal Complexes at Oxide Surface*, Journal of Colloid and Interface Science, 1997.
3. Doremus, R. H. and F. Alim-Marvasti, *The Rate of Dissolution of Amorphous Silica in Water*, Rensselaer Polytechnic Institute, Troy.
4. Gates, Bruce, *Catalytic Chemistry*, John Whiley & Sons, Inc., New York, 1992.
5. Park, Jaehyeon, *The pH Buffering Effect and Charging Behavior of Oxides in Aqueous Solution*, Heckman Binery Inc., Chicago, 1995.
6. Park, Jaehyeon and John Regalbuto, *A Simple, Accurate Determination of Oxide PZC and the Strong Buffering Effect of Oxide Surfaces at Incipient Wetness*, Journal of Colloid and Interface Science, 1995.
7. Schreier, Marc, *A Theoretical Study on CO_2 Solubility in Water as a Function of pH.*
8. Tamura, Hiroki, Akio Tanaka, Ken-ya Mita, and Ryusaburo Furuichi, *Surface Hydroxyl Site Densities on Metal Oxides as a Measure for the Ion-Exchange Capacity*, Journal of Colloid and Interface Science, Sapporo, 1998.

EXAMPLE SHEETS OF MathCAD PROGRAM

γ-ALUMINA SL = 6,000 m^2/L

RPA Model Calculations

Defined Unit Values

$nm := 10^{-9}m \qquad M := 1\frac{mol}{L}$

Variables

$\varepsilon := 78.41 \qquad c_o := 1M \qquad \Delta pK := 4.0$

$V_{sample} := 0.05L$

$O_{added} := 1.2gm$

$M_{ionic} := 0.1M$ Since we are using a 1:1 electrolyte, the molarity is equal to the ionic strength.

$s_{areaO} := 250\frac{m^2}{gm}$

$z_{pos} := 1 \qquad z_{neg} := 1$ Note, here the absolute value is used.

$PZC := 8.5$

Fixed values for the RPA Calculations

$k := 1.3806610^{-23}\frac{J}{K}$

$T := 298K$

$\eta := 1.6\cdot 10^{-19}C$

$F := 9.64910^{4}\frac{C}{mol}$

$N_s := 8.0\frac{1}{(nm^2)}$

$\varepsilon_o := 8.85410^{-12}\frac{C^2}{N\cdot m^2}$

$A := 6.02210^{23}\frac{1}{mol}$

Equations

$$\Gamma_t := \frac{N_s}{A}$$

$$\Gamma_t = 1.328 \times 10^{-5} \frac{mol}{m^2}$$

$$n_o := M_{ionic} \cdot A$$

$$n_o = 6.022 \times 10^{22} \frac{1}{L}$$

$$w := \frac{O_{added}}{V_{sample}}$$

$$w = 24 \frac{gm}{L}$$

Debye-Huckel Equation

$$f := 1\sqrt{M}$$

$$\gamma := 10^{\left[\frac{\left(-0.51 z_{pos} \cdot z_{neg} \cdot \sqrt{M_{ionic}}\right)}{f + \sqrt{M_{ionic}}}\right]}$$

Note, in order for the units to cancel properly in this equation, the number 1 is given units.

$$K_1 := 10^{-\left(PZC - \frac{1}{2} \cdot \Delta pK\right)_M}$$

$$K_2 := 10^{-\left(PZC + \frac{1}{2} \cdot \Delta pK\right)_M}$$

Initial Guess

$\Psi_o := 100\text{mV}$ $\sigma_o := 0.1\frac{C}{m^2}$ $Hf := 10^{-12}M$

Given

$$\sigma_o = \frac{F}{w \cdot s_{areaO}}\left[\left[10^{-pH}M - 10^{-(14-pH)}M\right] + \left(\frac{10^{-14}M}{Hf} - \frac{Hf}{M}\right)\cdot\left(\frac{c_o}{\gamma}\right)\right]$$

$Hf > 0$

$$\sigma_o = \sqrt{8\cdot\varepsilon\cdot\varepsilon_o\cdot k\cdot T\cdot n_o}\cdot\sinh\left(\frac{\eta\cdot\Psi_o}{2\cdot k\cdot T}\right)$$

$$\sigma_o = \left[\frac{\frac{Hf\cdot e^{-\frac{\eta\cdot\Psi_o}{k\cdot T}}}{K_1} - \frac{K_2\cdot e^{\frac{\eta\cdot\Psi_o}{k\cdot T}}}{Hf}}{\left(\frac{Hf\cdot e^{-\frac{\eta\cdot\Psi_o}{k\cdot T}}}{K_1} + 1 + \frac{K_2\cdot e^{\frac{\eta\cdot\Psi_o}{k\cdot T}}}{Hf}\right)}\right]\cdot F\cdot\Gamma_t$$

$H(pH) := \text{Minerr}(\Psi_o, \sigma_o, Hf)$